Applied Physics Reviews

Doping challenges and pathways to industrial scalability of III–V nanowire arrays

Cite as: Appl. Phys. Rev. **8**, 011304 (2021); https://doi.org/10.1063/5.0031549
Submitted: 02 October 2020 . Accepted: 15 December 2020 . Published Online: 12 January 2021

Wonjong Kim, Lucas Güniat, Anna Fontcuberta i Morral, and Valerio Piazza

COLLECTIONS

F This paper was selected as Featured

ARTICLES YOU MAY BE INTERESTED IN

Hybrid printed three-dimensionally integrated micro-supercapacitors for compact on-chip application
Applied Physics Reviews **8**, 011401 (2021); https://doi.org/10.1063/5.0028210

Noise spectroscopy of molecular electronic junctions
Applied Physics Reviews **8**, 011303 (2021); https://doi.org/10.1063/5.0027602

Sodium-storage behavior of electron-rich element-doped amorphous carbon
Applied Physics Reviews **8**, 011402 (2021); https://doi.org/10.1063/5.0029686

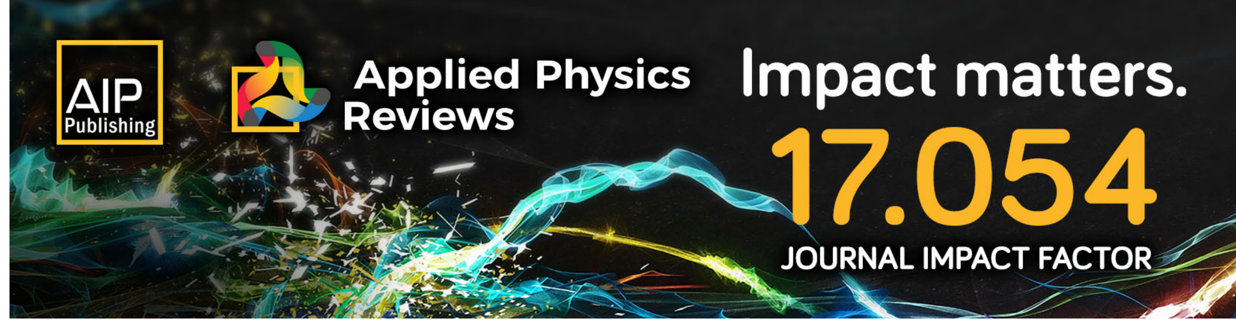

© 2021 Author(s).

Applied Physics Reviews REVIEW scitation.org/journal/are

Doping challenges and pathways to industrial scalability of III–V nanowire arrays

Cite as: Appl. Phys. Rev. **8**, 011304 (2021); doi: 10.1063/5.0031549
Submitted: 2 October 2020 · Accepted: 15 December 2020 ·
Published Online: 12 January 2021

Wonjong Kim,[1] Lucas Güniat,[1] Anna Fontcuberta i Morral,[1,2,a)] and Valerio Piazza[1,b)]

AFFILIATIONS

[1]Laboratory of Semiconductor Materials, Institute of Materials, Faculty of Engineering, École Polytechnique Fédérale de Lausanne, 1015 Lausanne, Switzerland
[2]Institute of Physics, Faculty of Basic Sciences, École Polytechnique Fédérale de Lausanne, 1015 Lausanne, Switzerland

[a)]Electronic mail: anna.fontcuberta-morral@epfl.ch
[b)]Author to whom correspondence should be addressed: valerio.piazza@epfl.ch

ABSTRACT

Semiconductor nanowires (NWs) have been investigated for decades, but their application into commercial products is still difficult to achieve, with triggering causes related to the fabrication cost and structure complexity. Dopant control at the nanoscale greatly narrows their exploitation as components for device integration. In this context, doping appears the truly last missing piece of the puzzle for III–V NWs, for them to become commercially exploitable. In this paper, we review the doping of bottom up III–V NW arrays grown by molecular beam epitaxy and metal-organic vapor phase epitaxy, aiming to link materials science challenges with the critical aspect of device design. First, the doping methods and mechanisms are described, highlighting the differences between self-assembled and ordered NW arrays. Then, a brief overview of the available tools for investigating the doping is offered to understand the common strategies used for doping characterization. Both aspects are crucial to discuss the recent advancements in reproducibility and up-scalability, which are discussed in view of large area fabrication for industrial production. Finally, the most common doping-related challenges are presented together with the latest solutions to achieve high performing NW-based devices. On this basis, we believe that new insights and innovative findings discussed herein will open the low dimensional materials era, on the premise of multidisciplinary collaborative works of all the sectors involved in the design and optimization of commercial products.

Published under license by AIP Publishing. https://doi.org/10.1063/5.0031549

TABLE OF CONTENTS

I. INTRODUCTION 1
II. DOPING MECHANISM IN NANOWIRES 2
III. CHARACTERIZATION METHODS 6
A. Structural characterization techniques 6
B. Electrical characterization techniques 8
C. Optical characterization techniques 8
D. Scanning characterization techniques 9
IV. THE CHALLENGE OF SCALABILITY 9
V. DEVICES AND RELATED CHALLENGES 10
A. Electrical junction in nanowire devices 10
B. Other doping related challenges 12
VI. CONCLUSION AND OUTLOOK 13
AUTHORS' CONTRIBUTIONS 13

I. INTRODUCTION

Despite its abundance and implementation in industrial processes, silicon shows some limitations for its future utilization in existing technologies such as solar cells and electronics.[1,2] III–V compound semiconductors are one of the most promising candidates to lead the post-silicon era with the additional ability to integrate the optoelectronic functionality. The use of III–V semiconductors is still limited at the industrial scale by the high cost of substrate materials and dedicated fabrication machines. Indeed, devices using high quality III–V materials require growth onto substrates with specific properties (in terms of lattice and polarity matching). This makes production extremely complex to develop and processes flexible hardly enough to account for a wide range of applications.[3–8] Recent progress in nanotechnology enabled the possibility to manipulate and structure matter almost to the atomic scale. It also provided the opportunity to realize new classes of functional devices based on nanostructures. Thanks to their small size, these structures exhibit much less limitations with respect to the substrate and can be integrated virtually onto any substrate ranging from silicon, diamond to van der Waals materials.[9–12] The implementation of III–V nanostructured devices could bring benefits at many levels: boosting performances in different technological areas,[13] monolithic integration of mismatched materials,[14,15] using

Published under license by AIP Publishing

reusable or economic substrates, and the reduction of production cost by reducing the amount of material into the devices. Among the III–V nanostructures explored in the last few decades, bottom-up nanowires (NWs) have stood out due to their inherent small lateral size, which effectively accommodates the strain stemmed from the lattice mismatch between different materials.[9,16,17] The layer-by-layer growth mechanism, together with the small footprint, also hinders the formation of antiphase boundaries resulting from the polarity mismatch with the substrate.[18,19] This advantage opened the way to monolithically combine III–V semiconductors with a less expensive substrate such as silicon, which would help also to smoothen the transition towards new generation devices.

For several decades, the potential of NWs grown by epitaxial methods has been demonstrated from their outstanding material quality to the realization of a large number of applications. It is, therefore, surprising that still today there is a substantial gap between NW-based laboratory-scale prototypes and commercially available products. The wide range of modern commercial electronics, as well as cutting-edge emerging technologies, is mainly based on well-established planar and top-down processes in the semiconductor industry. The question arises of what is required for bottom up NW systems to fulfill their promise and have widespread impacts. Despite the extensive work—theoretical and experimental—there are still some unanswered questions that limit their industrial applications.

In this context, NW doping has a central role. On one side, semiconductor doping is the key for tuning the properties of the active material in almost any electronic and optoelectronic device. On the other, it may strongly influence the growth mechanisms, the structure, and therefore the functional properties. As a consequence, the architecture and the design of the device as a whole and the final performance depend on the capability to control the dopant incorporation in the nanowires. Doping corresponds to the intentional minute introduction of foreign impurities in a semiconductor crystal to significantly modify its electrical, optical, and structural properties. The techniques used to introduce these impurities in nanowires are generally "*in situ*," indicating that the incorporation of dopants occurs simultaneously to the material synthesis. The introduction of dopants during synthesis may affect the physical mechanisms involved in the process. As a consequence, the synthesis parameters need to be adjusted in order to obtain the optimal result. Indeed, the optimization of the parameters is highly dependent on the chemical nature of the semiconductor and of the dopant species. This is discussed in Sec. II, where the growth mechanisms of doped nanowires are described in detail. Here, we will mainly focus on two epitaxial growth techniques, i.e., molecular beam epitaxy (MBE) and metal-organic vapor phase epitaxy (MOVPE), which are relevant to obtain III–V nanowires in a high quality and reliable manner. The overall picture is even more complex when considering the effect of doping impurities at the nanoscale. Indeed, when scaling down to few tens of nanometers, a tiny amount of dopant atoms can change drastically the properties of the semiconductor. For example, 10 phosphorous atoms into a 10 nm silicon cube yield a dopant concentration of 10^{19} cm^{-3}, which is considered to be a high doping level in semiconductor science.[20] In the other term, the doping concentration and distribution must be precisely characterized to obtain an ultra-fine control over the growth conditions and to produce high performing devices. In this perspective, doping characterization techniques (discussed in Sec. III) are a bridging point between materials science and device engineering.

Contrary to bulk and thin film semiconductors, bottom-up NW-based devices are composed of an ensemble of millions of individual nano-objects, called arrays. As the functional properties of such an array depend on the uniformity of the nanowire morphology and crystal quality, two of the most studied aspects in this field in the last 10 years are the growth reproducibility and the up-scalability. Recent progress indicators such as selective area growth (SAG), novel template-based approaches, and horizontal NW design aim to enable the growth of large area arrays composed of millions of ordered nanowires with identical properties. Achieving a reliable large area growth of identical nanowires would also directly impact the semiconductor manufacturing industry, paving the way for a full commercial exploitation of nanomaterials. Due to their relevance, these progress indicators will be reviewed in Sec. IV, where the impact of the up-scaling strategies on the doping uniformity is discussed. Finally, Sec. V will be devoted to the common doping-related challenges for the realization of highly performing NW-based devices. The concepts discussed in this section will help to underline the challenges to overcome along the path towards the commercialization of nanostructured electronics and opto-electronic devices. This involves a wide range of applications as summarized in Fig. 1. All these applications require a precise control of doping in a reproducible manner, and of course, scalability issues need to be addressed when it comes to device application to compete with the conventional planar devices in the market. It is not an easy task, but interdisciplinary collaborative work from modeling, growth, characterization, innovative device design, and fabrication can hopefully bring a low dimension material era in the near future.

Despite these challenges, the NW community has been dedicating a lot of effort and passion to master this topic, and comprehensive reviews on growth and doping are already available in the literature.[13,21–24] However, a significant gap still exists between the fundamental aspects and the practical realization of commercial products. In this paper, we aim to provide a comprehensive review, oriented to the production of NW-based devices as an ultimate technology to outdate silicon in the next future.

II. DOPING MECHANISM IN NANOWIRES

The most common mechanisms exploited for the growth of III–V NWs are the so-called vapor–liquid–solid (VLS), vapor–solid–solid (VSS), and vapor–solid (VS). In the former, a liquid/solid metal catalyst forms and preferentially gathers vapor precursors and generates an alloy. Once supersaturation of the components in the catalyst is reached, a solid phase precipitates at the bottom of the droplet, resulting in the one-dimensional growth of a NW.[25]

In VLS- and VSS-grown arrays, the position of the nanowires is determined by the location of the catalyst particles on the substrate. In the case where the droplet distribution is stochastic, long-range order cannot be obtained. This results in a difference in nucleation and incubation times arising from the droplet size dispersion, which usually leads to inhomogeneity in diameter and length. NW arrays of such a type are indicated as "self-assembled NWs." The VS technique, instead, is a catalyst-free growth method. In the context of NWs, it consists of a layer-by-layer growth on the substrate. As growth occurs in a highly kinetically dominated regime, the difference between growth speeds of different crystal planes will lead to an asymmetrical

Published under license by AIP Publishing

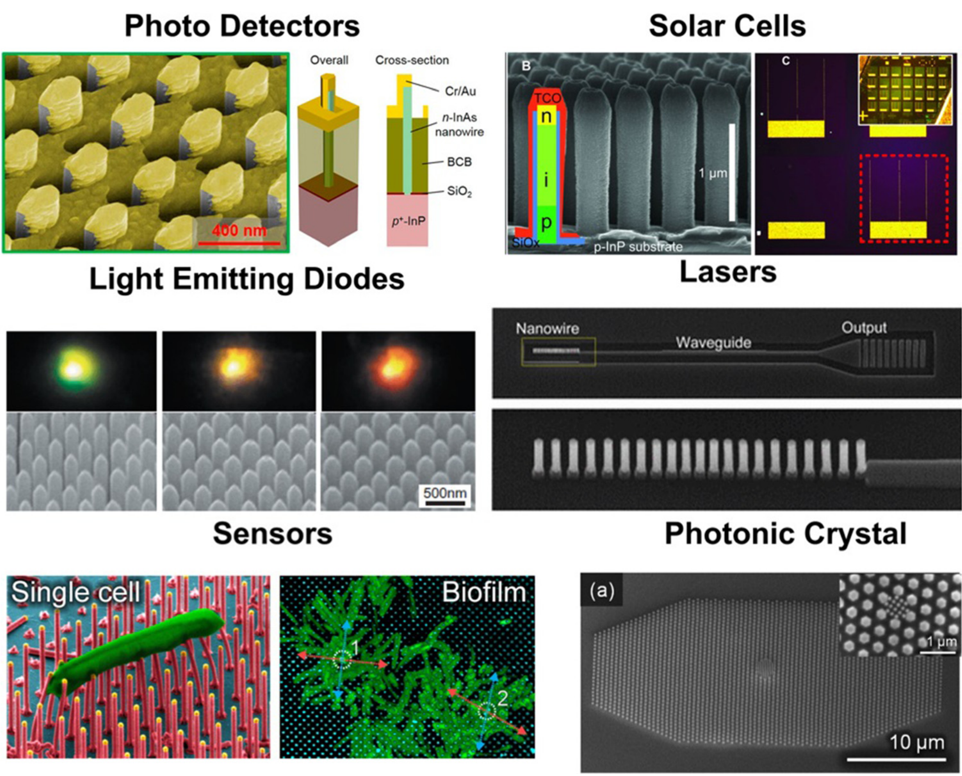

FIG. 1. Development of devices based on III–V nanowire arrays as interdisciplinary collaborative work from modeling, growth, characterization, innovative device design, and fabrication. Examples of devices currently under research: photodetectors [Adapted with permission from Ren *et al.*, Nano Lett. 18, 7901 (2018). Copyright 2018 American Chemical Society], solar cells [Adapted with permission from Wallentin *et al.*, Science 339, 1057 (2013). Copyright 2013 American Association for the Advancement of Science], light emitting diodes [Adapted with permission from Sekiguchi *et al.*, Appl. Phys. Lett. 96, 231104 (2010). Copyright 2010 AIP Publishing LLC], lasers [Adapted with permission from Kim *et al.*, Nano Lett. 16, 1833 (2016). Copyright 2017 American Chemical Society], sensors [Adapted with permission from Sahoo *et al.*, Nano Lett. 16, 4656 (2016). Copyright 2016 American Chemical Society.], photonic crystal [Adapted with permission from Scofield *et al.*, Nano Lett. 11, 2242 (2011). Copyright 2011 American Chemical Society].

crystal.[26,27] In the case of III–Vs such as GaAs or InAs, the (111) family of planes will govern the growth, and a mask opened in that direction will result in a vertical NW growth.[28]

Nanowire growth by a VS mechanism typically requires mask openings to obtain the desired morphology. As the shape and position of the openings on the surface can be easily controlled, a more uniform NW morphology can be achieved.

This method can be referred to "selective area epitaxy" (SAE), often corresponding to the fabrication of ordered NW arrays. Notably, the correlation between the growth mechanism, array ordering, and nanowire uniformity has weakened as new growth methods are constantly under development. For instance, Ga-catalyzed NWs grown on patterned substrates enable the growth of ordered NW arrays by VLS or VSS.[29–31] The same result was obtained by controlling the catalyst distribution on the substrate by nanoimprinting lithography.[32] It is worth mentioning that until now, ordered NW arrays have always been achieved through substrate patterning.

The growth mechanism strongly affects the incorporation of dopant atoms in nanowires. In both VLS- and VS-driven nanowire growth, the addition of a dopant may influence the thermodynamics and kinetics of the system as it may affect surface energies. The balance among the two affects the crystal growth and the dopant incorporation. Both thermodynamics and kinetics depend on the chemistry of the system, i.e., on the chemical nature of the substrate, III–V elements, and dopant species, not to mention temperature, partial pressures, and atomic fluxes. It is, thus, highly complex to generalize dopant incorporation for III–V NWs. The complexity of the topic can be appreciated from Table I, which shows a summary of reported dopant concentrations in binary III–V NWs, highlighting growth techniques and dopant elements.

Despite the myriad of details concerning elements, growth techniques, and the parameters used for doping, it is possible to unveil principles common to all the NW doping processes. Figure 2 depicts the main dopant incorporation paths in NWs, which are either through the catalyst (i.e., along the growth direction) or through the side facets. It is usual to see a contribution of both mechanisms during the catalyzed growth of III–V NWs.[23,33]

In the case of VLS, dopant incorporation through the catalyst occurs at the liquid–solid growth front interface.[34] The dopant concentration depends on the solubility of the dopant material in the catalyst and the segregation coefficient of the dopant material into the solid NW. Intuitively, this incorporation path affects the doping profile

Published under license by AIP Publishing

TABLE I. Reported binary III–V NWs with the dopant element and doping concentration range (in atoms·cm^{-3}).

Material	Growth method	n-type	p-type
AlN	MBE, CVD,[a] MOVPE	SiH_4[35] 6.7×10^{20} –2.4×10^{21}	Mg[36] 10^{16} $MgCl_2$[35,37,38] 4.4×10^{20} – 8.6×10^{21} Cp_2Mg[39] 1.2×10^{20} –7.7×10^{20}
GaN	MBE, MOVPE	Si[40–45] 3.0×10^{18}–2.7×10^{21} SiH_4[46–50] 10^{18}–10^{20}	Mg[41–45] 10^{17}–10^{20} Cp_2Mg[46–50] 10^{16}–3.0×10^{18} Mg_3N_2[51,52] 10^{17}–10^{20}
InN	MBE, MOVPE	Si[53–55] 5.0×10^{17}–1.1×10^{20}	Mg[55,56] 2.0×10^{15}–6.0×10^{15} DEZn[57] 2.0×10^{21}
GaP	MOVPE, sublimation	TESn[58] (N/A) DTBSe[58] (N/A) SiH_4[58] (N/A) S[59] 5.0×10^{20}	DEZn[58] (N/A) NH_3[60] 10^{18}
InP	MBE, MOVPE, LCG[b]	Si[61] 3.0×10^{17}–3.0×10^{18} SiH_4[62,63] 10^{18}–3.0×10^{18} H_2S[21,64–67] 3.0×10^{18} Te[68] 4.0×10^{20} TESn[70–74] 10^{17}–10^{19} Se[69,75,76] 2.0×10^{17}–10^{20}	Zn[68] 4.0×10^{20} Zn_3P_2[69] 1.2×10^{21} *DEZn*[4,6,63–66,71–73,77,78] 1.0×10^{17}–1.2×10^{20} *DMZn*[70] (N/A)
GaAs	MBE, MOVPE	Si[79–81] 10^{17}–10^{20} SiH_4[82] 3.5×10^{17} Si_2H_6[83–85] 10^{17}–5.0×10^{18} GaTe[89–91] 4.0×10^{18}–2.0×10^{19} TESn[92–94] 10^{18} –3.0×10^{18}	Si[80,81,86,87] 1.4×10^{18}–4.0×10^{19} C[83] 8.0×10^{18} DMZn[88] 10^{17} Be[81,90,91,95,96] 10^{18}–10^{21} DEZn[67,77,82,85,88,92–94,97] 10^{17}–2.3×10^{19}
InAs	MBE, MOVPE	TESn[98–100] 1.9×10^{18}–10^{19} $SiBr_4$[100] (N/A) DTBSe[99,100] 10^{18}–1.2×10^{20} SiH4[98] 6.8×10^{16} Si_2H_6[101] 10^{17}–3.9×10^{18} H_2S[100] 6.2×10^{17}–3.1×10^{18}	DEZn[98] (N/A) Be[102,103] 7.0×10^{17}–3.0×10^{18}
GaSb	MBE, CVD, MOVPE	Te[104] 1.7×10^{18}	Zn[105] (N/A)
InSb	CVD, MOVPE	N/A	C[106] 7.5×10^{17}

[a]Chemical vapor deposition.
[b]Laser-assisted catalytic growth.

Published under license by AIP Publishing

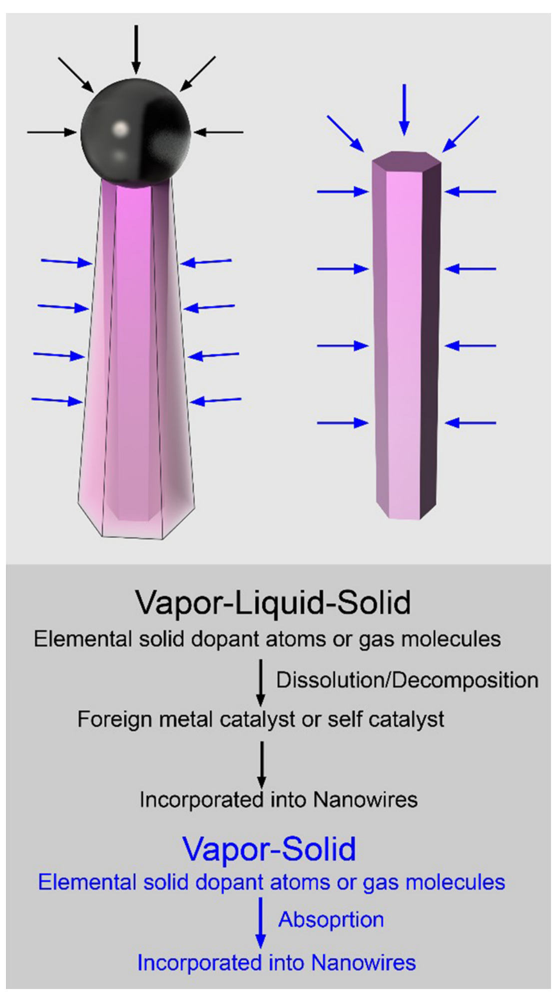

FIG. 2. Dopant incorporation paths in nanowires with VLS and VS mechanisms, respectively, through the catalyst (i.e., along the growth direction) or through the side facets. It is usual to see a contribution of both mechanisms during the catalyzed growth of III–V NWs, as shown on the left picture.

along the growth direction. At the same time, dopant incorporation through the side facets can occur. This process is mediated by the crystal orientation of different facets.[107]

If the two incorporation paths are not properly coordinated, inhomogeneities in dopant distribution can arise, with possible detrimental effects on the functional behavior of the nanowires to mitigate this issue, and growth conditions can be tuned in order to suppress one of the two paths, like introducing etching species.[108] Borgström *et al.* suppressed VS contribution by introducing HCl during the growth of Au catalyzed InP NWs in MOVPE. However, Connell *et al.*[109] reported that inhomogeneities can also arise during the sole incorporation through the droplet. Atom probe tomographic (APT) analysis on Au-catalyzed B-doped Si and P-doped Ge NWs revealed that dopants are preferentially incorporated near the VLS trijunction. The authors addressed the observed dopant anisotropy to the faceting of the liquid–solid growth interface.

Nonuniform dopant distributions in NWs are also observed in different material systems, although controversial reports can be found. An example is the incorporation of dopants in MBE grown self-catalyzed GaAs NWs. Preferential incorporation of Be atoms along threefold symmetric truncated facets under a liquid Ga catalyst has been reported by off-axis electron holographic analysis.[110] The dopant diffusion into the NW core during the process leads to the radial and azimuthal variations of dopant distribution. On the contrary, Zhang *et al.* reported a uniform Be dopant distribution both along the length of the NWs and radially across the diameter in the same material system.[111] Also, Te dopant incorporation has been studied using several complementary techniques.[89] Models show that Te is mainly incorporated by the VLS process through the Ga catalyst, which results in both axial and radial dopant gradients due to Te diffusion inside the NWs and competition between axial elongation and radial growth of NWs. By comparing Raman spectroscopy and APT analysis, they demonstrated that the activation of Te donor atoms is 100% at a doping level of $4 \times 10^{18}\ \mathrm{cm}^{-3}$.

The amphoteric nature of the Si doped GaAs NWs (one of the most studied systems in III–V NW doping) brings an additional element to consider.[80,81,86,87] In particular, it has been shown that Si incorporates mainly in As-sites in Ga-assisted growth. For concentrations higher than few $10^{18}\ \mathrm{cm}^{-3}$, Si atoms drive Si-Si pair formation, resulting in doping compensation.[86] In 2019, Hijazi *et al.* presented a model elucidating the importance of catalyst droplet composition as a function of temperature, which allows for better understanding of Si doping of Au catalyzed and self-catalyzed GaAs NWs.[112] They explained why most VLS Si-doped GaAs NWs are p-type and demonstrated n-type Si doping of Au-catalyzed GaAs NWs grown by hydride vapor phase epitaxy (HVPE) using high As concentration in the liquid Au catalyst. Furthermore, very recently, Dubrovskii *et al.* pointed out that the III–V VLS NW doping process is sensitive to the chemical potential oscillations related to depletion of group V atoms in a catalyst droplet using the analytic model, which quantifies the doping oscillation over the monolayer formation cycle.[113]

Using a solid metal catalyst, vapor-solid-solid (VSS) NW growth may result in a more controllable doping process[114] due to reduced solubility of growth precursors, as well as dopant elements in the catalyst. In this case, the achievable doping level might be compromised. The trade-off between improved control and maximum doping concentration achievable needs to be evaluated to determine whether VSS growth is a valid option for the desired nanowire system.

One can consider removing the metal catalyst and to obtain homogeneous doping profiles in VS-grown NWs. In the case of particle-free growth, facet-dependent dopant incorporation can be present (as multiple crystal facets are growing simultaneously), thus leading to uneven doping profiles. In addition, typically VS-grown NW presents heavily defective crystal structures, which might be detrimental for electrical functionalities. Few post-growth processes such as etching[115] and thermal annealing[116] have been successfully applied to modify the electrical properties at the micrometer-scale. Their use to tune doping at the atomic level in future is unlikely as they are not controllable at this scale.

Control over the dopant distribution down to the monolayer represents one key to unlock the use of III–V nanowires in a wide range of applications. Unfortunately, unveiling the complicated nature of NW doping is not an easy task. The majority of the studies were so far

Published under license by AIP Publishing

conducted on self-assembled nanowires. As self-assembled growth is inherently indeterministic, it leads to an intrinsic statistical uncertainty. When NWs are randomly positioned on the substrates, each has a different surrounding during the growth, and the adatom collection area is, therefore, affected. The consequent variation of their morphologies, composition, and structural properties can also provide significant instabilities to the dopant distribution. Therefore, the great potential of NW arrays can only be relevant if we master NW doping in ordered array systems. In this perspective, position-controlled ordered NW arrays are essential for systematic doping studies.

To the best of our knowledge, the effects of doping in ordered array systems have not been fully investigated yet. However, thanks to the recent advances in ordered NW growth,[31] their use for studying and engineering NW doping in a more systematic manner is expected. The possibility to exploit ordered arrays of nanowires will help disclosing the relation between the growth mechanism and dopant incorporation.

It will be interesting to see how doping studies on ordered nanowire arrays will affect the current understanding of surface driven effects such as depletion, dopant deactivation, and Fermi level pinning. As device dimensions are scaled down, the surrounding surface of the semiconductor will become more important and will possibly rule the electronic properties.

For example, in 2009, IBM demonstrated the discrepancy between the physical radius and electronic radius of NWs.[117] They presented the effect of doping deactivation by measuring the electric conduction of phosphorous doped Si NWs as a function of radius, temperature, and dielectric surrounding. The increase in ionization energy with the decreasing nanowire radius proved the effect of surface states and dielectric mismatch. This effect is even more pronounced in GaAs, which has very high surface recombination velocity compared to other III–V semiconductors. Chang *et al.* calculated free carrier density as a function of doping concentration for GaAs NWs with various diameters.[118]

When the doping concentration is below 10^{17} cm^{-3}, NWs are fully depleted at the diameter of 100 nm. Indeed, this phenomenon has a significant impact on the functional properties of individual NWs and therefore on the development of nanowire-based devices. In this context, arrays made of millions of identical NWs are a precious platform for the doping studies in the next future.

As a small amount of dopant can drastically change the growth dynamics,[77,78] accurate characterization of dopant concentration is necessary. For this reason, Sec. III will discuss available doping characterization methods, highlighting their strength, weaknesses, and complementary nature.

III. CHARACTERIZATION METHODS

A large range of methods have been used to characterize bulk and thin film semiconductors.[119–121] The use of these techniques to probe nanostructures, such as nanowires, involves several challenges. On one side, the reduced dimensions and material volume require techniques with high sensitivity. On the other, a very high spatial resolution is necessary to reveal the physics of the dopant incorporation and its relation to the growth mechanisms. At the same time, dopant distribution affects the electrical properties, i.e., due to the amplified effect of surfaces in depleting carriers.[122,123] In this regard, doping analysis and interface engineering are fundamental for the future development of nanowire-based devices.

To account for this complex picture, doping investigations in III–V nanowires are usually approached by multi-scale methods, which require high spatial resolution and chemical/electrical/optical sensitivity. This strategy aims to tackle the task by obtaining information at different scales and/or on different doping-related properties, ideally on the same nanowire.[124]

Analysis on multiple nanowires or on nanowire arrays can also be performed. In this case, the result is considered an average over the ensemble. For this type of measurement, SAE nanowire arrays, which are expected to yield a higher uniformity, are preferable over self-assembled ones.[8,125,126] This may be highly helpful also for the development of nanowire-based devices in the near future as high uniformity have to be ensured also to obtain a reliable device on a large scale surface.[127]

This section reviews several methods used to characterize the doping in semiconductor nanowires. The discussed techniques are given in Subsections III A–III D to emphasize similarity, differences, advantages, and disadvantages of each of them. We believe that the following classification is highly beneficial to readers interested in particular doping-related issues.

A. Structural characterization techniques

The most intuitive strategy to characterize the doping of semiconductor materials relies on the analysis of the chemical nature and position of the dopants. The identification and mapping of atoms in bulk or thin film materials have traditionally been performed by energy-dispersive x-ray spectroscopy (EDX), secondary ion mass spectroscopy (SIMS), and, more recently, atom probe tomography (APT).

These techniques are characterized by very high chemical selectivity and high spatial resolution, enabling us to obtain elemental data and/or maps concerning the composition of the probed material.

The main difference among these techniques is related to the limit of detection (i.e., the minimum detectable quantity of a given species). This is the most important parameters when investigating the doping by this kind of techniques. As an example, considering that in 1 cm^3 of GaAs are present roughly 10^{22} atoms, a limit of detection of at least 0.001% is necessary to detect dopant concentrations on the order of 10^{17} cm^{-3}. This is the main reason why EDX, extensively used in semiconductor technology, is poorly suited for doping analysis in III–V nanowires: due to its high limit of detection (around 0.1% in the best conditions[128]), it has been used only for microwires where a very high dopant concentration was expected.[129]

SIMS is better-suited for the purpose.[130,131] Standard time-of-flight (ToF) SIMS measurements can detect concentrations as low as 10^{17} cm^{-3} in thin films.[132] Its nanoscale version exhibits high spatial resolution (∼ 50 nm lateral resolution and ∼ 20 nm depth resolution),[133,134] which makes it highly suitable for the investigation of NWs.[135] An example is the work of Chia and coauthors[136] on MBE grown Au-catalyzed GaAs NWs, where doping profiles for n- and p-dopants have been measured [Fig. 3(a)]. The results lead to key insights into the growth mechanisms with useful feedback for the device design.

Although nano-SIMS is a powerful tool to probe individual NWs, it is less suited to map the dopant distribution in specific

Published under license by AIP Publishing

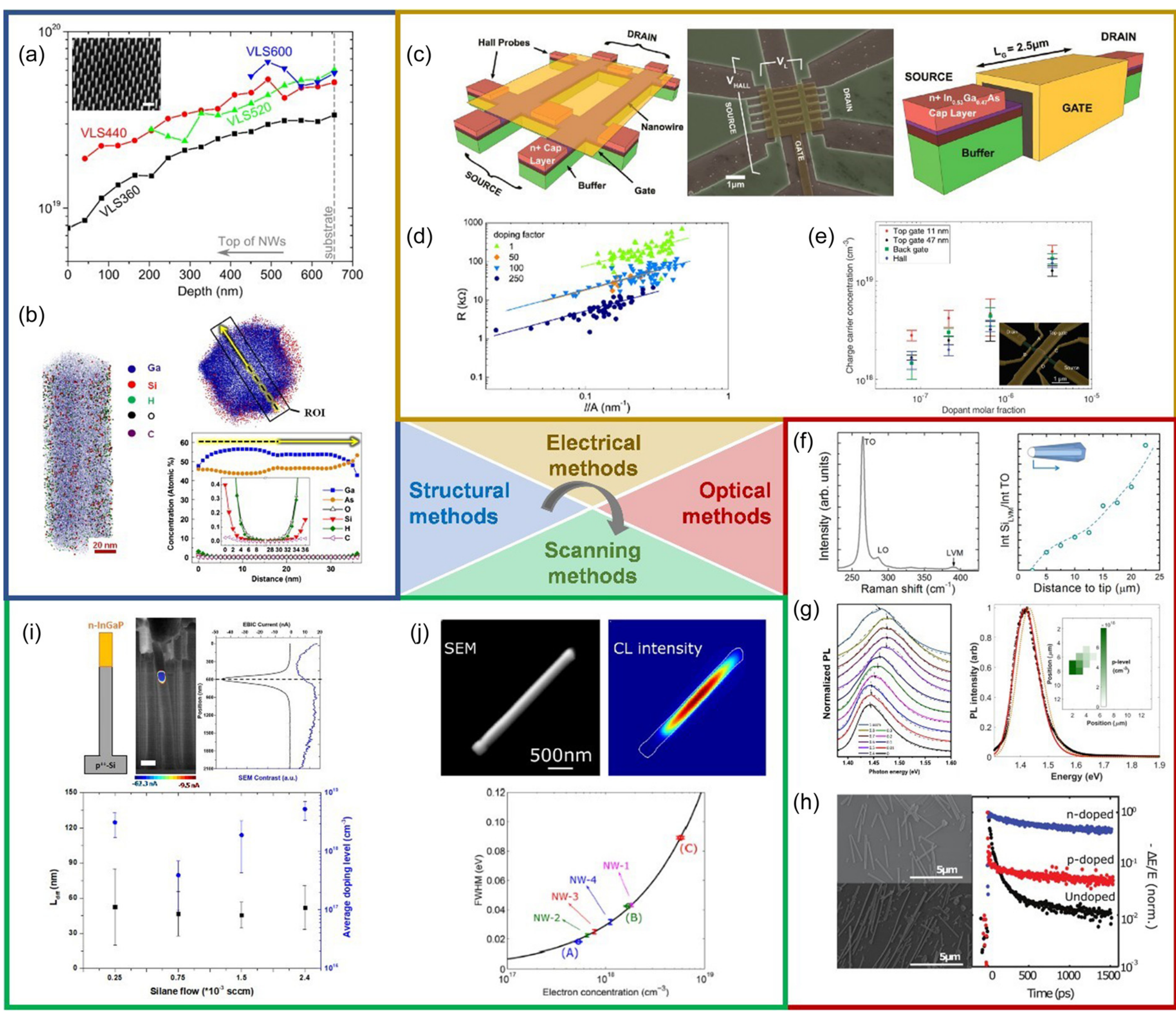

FIG. 3. Examples of doping characterization done by structural (blue-framed), electrical (yellow-framed), optical (red-framed), and scanning probe (green-framed) methods. In the center is a visual guide to the figure. The gray arrow indicates the order these methods are discussed in the text and the labeling. (a) SIMS: dopant concentration as a function of depth for different Be:GaAs NWs. In the inset, a SEM image of the as-grown array. Adapted with permission from Chia *et al.*, J. Appl. Phys. 118, 114306 (2015). Copyright 2015 AIP Publishing LLC. (b) APT: on the left, 3D reconstruction of a NW with Ga atoms, Si dopants and contamination elements H, O, and C mappings; on the right, 2D atoms distribution map of the Ga and Si and 1D radial relative composition profile of Si dopants and contamination elements. Adapted with permission from Ren *et al.,* Appl. Phys. Lett. 107, 022107 (2015). Copyright 2013 Elsevier B.V. (c) Schematic and SEM image of a micro-system for resistivity, FE and Hall effect measurements. Adapted with permission from Thathachary *et al.*, Nano Lett. 14, 626 (2014). Copyright 2014 American Chemical Society. (d) Resistivity measurements: four-points resistance of Si:InAs NWs as a function of the distance of metal contact to the cross section ratio (l/A) for nanowires with a different doping (color-coded). The straight lines correspond to the linear fits for each doping factor Adapted with permission from Wirths *et al*., J. Appl. Phys. 110, 053709 (2011). Copyright 2011 AIP Publishing LLC. (e) FE and Hall measurements: charge carrier concentrations in S:InP as a function of dopant gas molar fraction used during the growth. The error bars show the standard deviation within the measured NWs. In the inset, the SEM image of the measurement micro-system. Adapted with permission from Hultin *et al*., Nano Lett. 16, 205 (2016). Copyright 2016 American Chemical Society. (f) Raman spectroscopy: on the left, the Raman spectrum of a single Si:GaAs nanowire. The vibrational mode at 393 cm^{-1} corresponds to the incorporation of silicon in arsenic sites. On the right, the spatial distribution of the dopant concentration defined by the intensity ratio between the LVM and TO modes along the nanowire. Adapted with permission from Dufouleur *et al*., Nano Lett. 10, 1734 (2010).Copyright 2010 American Chemical Society. (g) PL: on the left, the spectra of Si:GaAs nanowire arrays grown under various dopant flow rates. Adapted with permission from Arab *et al*., Appl. Phys. Lett. 108, 182106 (2016). Copyright 2016 AIP Publishing LLC. On the right, the PL spectrum of a single Zn:GaAs NW and related fitting (red line). The predicted PL from undoped GaAs is given by the orange dotted curve, demonstrating the PL redshift due to doping. The inset shows a p-doping map for this nanowire. Adapted with permission from Alanis *et al*., Nano Lett. 19, 362 (2019). Copyright 2019 American Chemical Society. (h) THz spectroscopy: on the left, SEM images for Si- (top) and C- (bottom) doped GaAs core-shell NWs. On the right, comparison of the decay of normalized photoconductivity for n-type (blue) and p-type (red) doped nanowires with an undoped nanowire reference sample (black). Adapted with permission from Boland *et al*., ACS Nano 10, 4219 (2016). Copyright 2016 American Chemical Society. (i) EBIC: on top, schematic of Si:InGaP NWs on B:Si stems, EBIC map, and corresponding EBIC current profile along the longitudinal axis. On the bottom, doping estimation as a function of the dopant flow used during the growth. Adapted with permission from Piazza *et al*., Appl. Phys. Lett. 114, 103101 (2019). Copyright 2019 AIP Publishing LLC. (j) CL: on top, SEM image, and corresponding CL map of a single Si:GaAs NW. On the bottom, FWHM extracted form CL measurement as a function of the carrier concentration for different doping levels. Adapted with permission from Chen *et al*., Nano Lett. 17, 6667 (2017). Copyright 2017 American Chemical Society.

locations, i.e., interfaces, since a much lower limit of detection and a spatial resolution on the order of nm are necessary.

Interface engineering is critical in view of commercial devices: for example, it is key to control the dopant incorporation down to the monolayer to estimate the sharpness of an electrical junction and for the study of quantum objects embedded in NWs. Novel advances in SIMS such as 1.5D and self-focusing SIMS show promise to tackle these problems.[134]

More commonly, these challenges are addressed by APT, which provides a very high spatial resolution ($\sim$ 1 nm, Ref. 137) and a lower limit of detection (roughly $10^{16}\,\mathrm{cm}^{-3}$).[138] Therefore, APT is strongly favorable for the analysis of atomic distributions in NWs.[139–141] Agrawal *et al.*[142] used this method to measure the distribution of Mg atoms in high bandgap III–V NWs, obtaining both axial and radial maps. The technique has been subsequently refined, enabling full 3D volume reconstruction, as in the work of Du and coauthors [Fig. 3(b)].[143] The main drawback of this method is that both sample preparation and data acquisition and analysis are highly time-consuming. For this reason, a systematic analysis of an entire NW array is virtually impossible, at the moment. Still, APT is highly valuable, especially in combination with other techniques. This strategy allowed us to describe the incorporation of dopants and to have a deep understanding of the physical phenomena occurring in NWs.[89,144]

Last but not least, it is worth noting that all the structural characterization techniques imply a risk of permanently damaging the investigated material and can be thus of destructive nature. In this case, they cannot be simultaneously performed on the same position, thus limiting their execution on the same nanowire.

B. Electrical characterization techniques

Semiconductor doping aims to engineer the conductivity—or more generally the electrical properties—of semiconductors. It is, therefore, natural to analyze the electrical properties to characterize the carrier concentration and mobility to investigate the doping efficiency. This strategy is commonly used for thin film technologies where electrical techniques are routine methods to assess the doping concentration. The adaptation to the nanoscale was enabled by the advancements in nanofabrication of test structures for single nanowire analysis.[145,146] A flawless fabrication is crucial since the contacts define the access of charge carriers to the material [Fig. 3(c)].[87,147,148]

Current-voltage and field effect (FE) measurements are often exploited in combination [Fig. 3(d)] to estimate the average carrier concentration and mobility in nanowires. The former, performed in 2-points and/or in 4-points configurations, enables the assessment of the resistivity, while the latter allows us to assess the charge type and the carrier concentration by monitoring the variation of the source-drain current as a function of the gate voltage.[101,149] Combining the data, also the charge mobility can be estimated using Drude-like models, potentially enabling a full characterization of the transport properties in single NWs.

An alternative to FE measurements is to perform Hall measurements. In this type of analysis, the Lorentz-type interaction between the current flowing in the NW and a perpendicular magnetic field leads to the build-up of an electric potential, which can be easily related to the carrier concentration.[148,150]

The accuracy of the values obtained through these electrical characterization methods is intimately related to the reliability of the parameters to be used in the models describing the current-voltage dependence.[151] For example, capacitance values are usually difficult to estimate due to their dependence on surface and bulk properties, as well as on the nanowire-gate geometry.[152,153] As a result, charge trapping at the surface is often neglected, and I-V or C-V hysteresis is under-reported. The difficulty in including these phenomena in a theoretical or semi-empirical model may represent the main sources of error in doping estimation. Hultin *et al.*[154] compared FE and Hall measurements on S-doped InP NWs. In their study, the authors conclude that FE measurements are more sensitive to the surface properties, while Hall measurements give a better estimation of the bulk properties. They highlight the significant impact of the electrical modeling of the nanowire. Still, in this study, the carrier concentration obtained with the two techniques differ only slightly [Fig. 3(e)].

Among other electrical methods, recently, techniques based on thermoelectric effects have been developed, although less commonly used for the analysis of III–V nanowires.[144,155] For a more technical description of the conventional electrical characterization techniques for semiconductor materials, please refer to Ref. 156.

C. Optical characterization techniques

Material research involves several cycles of design, growth, characterization, and analysis in order to achieve high-quality results. This is even more important when developing nanostructured materials since the interplay of many factors plays a fundamental role during the growth. In this context, rapid characterization techniques on the as-grown material are highly desirable. Optical characterization typically falls in this category.

The most commonly used techniques are Raman spectroscopy, photoluminescence (PL), and optical-pump THz spectroscopy. Raman spectroscopy relates the vibrational modes of the crystal with the presence of impurities and therefore can be a sensitive to the concentration of dopants, when the local vibrational modes, LVMs, are Raman active. An estimation of the dopant density can be obtained by comparing the intensity of the LVM peaks.[86,157] In Si doped p-type GaAs, this approach can ensure a sensitivity around $10^{18}\,\mathrm{cm}^{-3}$ at best.

However, due to the non-destructive nature and absence of time-consuming sample preparation, Raman is widely used to study as grown-nanowire arrays. For example, it was used on GaAs microwires to study the incorporation of the dopant along the length of the nanowires[86,158] [Fig. 3(f)]. Also, more complex doping-related phenomena were studied, such as the amphoteric nature of Si atoms in GaAs NWs.[86,159]

Similarly, PL is widely used to investigate nanowires. The working principle of PL analysis relies on the inter-band transition of carriers under optical excitation and subsequent radiative recombination. Hence, this technique is used to study the incorporation of dopants in the material, which leads to the formation of intragap states and to an increase in the population in the conduction or valence band. Experimentally, the presence of dopant states results in a broadening and shifts of the luminescence peaks (such as bandgap narrowing and Burstein-Moss shift), dependent on the doping concentration[160–162] [Fig. 3(g)]. Thanks to the extensive literature on this topic, quantitative estimation of the doping concentration can be obtained by analyzing the shift in the luminescence spectra, with sensitivity up to $\sim 10^{17}\,\mathrm{cm}^{-3}$, enabling its use for systematic studies. For example, Arab *et al.* investigated the incorporation of

Published under license by AIP Publishing

Si in GaAs nanowires grown by metalorganic chemical vapor deposition (MOCVD) by relating the dopant flow used during the growth to the carrier concentration in the nanowires.[163] On a more applicative note, μ-PL maps were also use to evaluate the effect of the p-doping level on the lasing properties of GaAs nanowires.[164]

Raman spectroscopy and PL analysis can be used efficiently together to study III–V NWs by probing the impurity concentration and the resulting electronic structure.[157] Despite their easy implementation, both techniques are strongly limited in spatial resolution due to the excitation wavelength on the order of few hundreds of nm. For this reason, optical characterization methods are used mainly to investigate nanowire arrays, although a few analyses on single nanowires can be found in dedicated studies.[76,158]

Another established method is optical-pump terahertz spectroscopy, where the collective oscillation of free charges is excited, enabling the estimation of the doping concentration from complex conductivity spectra [Fig. 3(h)].[165] III–V NW ensembles have been investigated through this technique to retrieve not only the doping concentration but also material parameters such as carrier lifetimes, mobilities, and surface recombination velocities.[166] In this field, it is indeed worth mentioning the work of Herz and coauthors to investigate unintentional and intentional doping levels in InAs, InP, GaAs, and InAsSb NWs.[167–171]

D. Scanning characterization techniques

Scanning probe characterization techniques respond to the need to investigate a large number of nano-objects with high spatial resolution by combining nanometric probes (such as an electron beam) and scanning over macroscopic areas. When applied to doping analysis, this category of experimental tools finds their major advantages in the possibility to perform large statistical analysis with poor (or even without any) nanofabrication.[49,172,173] An example is given by electron beam induced current mapping (EBIC), extensively used for both thin films and nanostructured semiconductor analyses.[174,175] EBIC enables us to correlate the charges excited by the electron beam with the electronic band structure of nanowires containing electrical junctions.[176,177] This technique has been largely used on III–V NWs not only to determine the type of doping obtained with a given dopant species[178] but also to perform quantitative doping estimation across p-n junctions [Fig. 3(i)],[179] with a limit of detection of roughly $10^{17}\,cm^{-3}$. EBIC can be used also to investigate doping-related phenomena such as metal/semiconductor Schottky coupling and depletion regions in electrical junctions, which are fundamental for the development of optoelectronic devices.[73,181–183] An additional technique is cathodoluminescence (CL).

Contrary to EBIC, CL does not require the presence of a rectifying interface to enable material analysis since it relies on the interband transitions occurring under electron beam excitation.[184–186] In the case of doping, the analysis of data is extremely complex, and it requires a thin film calibration sample, enabling a comparative estimation. Nevertheless, reliable values of carrier density can be obtained, as demonstrated by the work of Lindgren and coauthors,[187] who showed a consistent agreement with Hall measurements. More recently, Chen *et al.*[180] developed a data analysis method relying on a spatial integration of the CL signal to define the peak position and FWHM representative of the carrier concentration in Si:GaAs NWs [Fig. 3(j)]. Additional scanning techniques have been developed and refined over the last few years. Indeed, electron holography is recently gaining a lot of consideration into the research community due to the possibility to combine structural analysis and electrical potential mapping at the very nanoscale (spatial resolution, $\sim$ 1 nm),[188] although several challenges related to surface states still need to be addressed to obtain a quantitative doping estimation.[124]

Other techniques such as scanning microwave impedance microscopy (SMIM) and x-ray fluorescence (XRF) are used in dedicated studies,[189,190] and progressive improvements are expected in the years to come.

IV. THE CHALLENGE OF SCALABILITY

Currently, a systematic functional analysis of each individual nanowire in a NW array is virtually impossible. The question is whether this is necessary, especially if all NWs would be identical. Self-assembled nanowires exhibit a relatively large NW size distribution, especially compared to position-controlled NW array systems. This is due partially to the variance in the interwire distance,[191] which in turn results in a fluctuation of the local precursor partial pressures.[30] Conductive AFM performed on self-assembled GaAs NW arrays and compared to top-down nanowire structures clearly illustrate this phenomenon.[127] In the self-assembled system, adjacent p-n NW junctions can exhibit significant differences in their electrical behavior, ranging from linear to diode-like characteristics. These variations have been attributed to a change in the doping concentration and/or distribution along the wire. In ordered arrays, the position of the NWs is determined by the substrate patterning. Consequently, a higher degree of similarity in the morphology is found, although NWs are not all identical in length and diameter.[30,192] Surprisingly, recent works indicate that the electrical properties may also vary considerably in well-ordered arrays.

All these raise questions concerning the scalability of NW doping: do we understand where inhomogeneities come from and can we find our way around them?

Concerning freestanding NW growth, it is known that the geometrical parameters of an array (i.e., interwire distance and hole size) can have an impact on the morphology and crystal structure of NWs due to the variation of the adatom flux, resulting in different local values of V/III ratio.[193–196] A variation in the precursor flux implies also a relative modification of the local dopant flux.

Morphological variations can also lead to variations in the dopant concentration and thus nonuniformity from NW to NW. One can consider that for NWs with a reduced size and low nominal doping levels, a fluctuation of few dopant atoms can lead to strong variations in their concentration. Moreover, the so-called "edge effect" contributes to the overall inhomogeneity. As NWs grow closer to the edge of a regular array, an additional adatom flux through diffusion from the dielectric mask can increase the NW growth rate. Non-linear position dependent NW growth dynamics[191,197] increases the complexity in dopant incorporation and junction parameter designs. In the context of a p-n junction, a difference in the axial and radial growth rate will lead to electrical junction inhomogeneities between the center and edge of an array. This effect could be more pronounced for an axially defined junction because a non-intentional radial growth will potentially decrease the junction performance by short circuiting the junction.

Published under license by AIP Publishing

However, one can imagine to take advantage of different axial and radial growth rates by obtaining NWs of different sizes on purpose to enhance light absorption.[198] One could, for example, integrate NWs with different heights and diameters in the same array, to absorb light more efficiently and increase the internal efficiency of a solar cell[199] as illustrated in Fig. 4(a). The suggested multiterminal NW solar cell device scheme is based on three different dimensions and compositions of III–V NWs as a unit cell, which enables an efficient lateral solar spectrum splitting.

Scalability issues are often considered as an important factor for bringing a device concept to the market. Considering that both MBE and MOCVD techniques are currently capable of producing high quality epitaxial films on industry scale 300 mm wafers, the scalable nanopatterning process gains significant importance. There are many different kinds of nanopatterning techniques, and a comprehensive review on recent progress of top-down lithography techniques is available in the literature.[200] Among different techniques, e-beam lithography (EBL) is the most widely used method for defining nanoscale features due to its high-precision and versatile nature. However, it is not yet appropriate for a large and dense area patterning due to low throughput and high cost. EBL-free patterning can bring a huge impact on the community, but still there is nothing can stand comparison with EBL when it comes to resolution and reproducibility. From the perspective of doping, horizontal NW configuration makes them very attractive compared to the vertical NW configuration in terms of scalability because the well-established planar doping process can be directly transferred and facilitate post-device fabrication processes on the original substrate.

In domains of application such as quantum computing[202] or photodetectors[203] where the number and density of devices on a chip are relatively low, up-scalability can be achieved either by the horizontally defined in-plane selective-area growth (SAG) technique using a template or mask to selectively grow one semiconductor material on top of another[204–210] or using dielectric templates that are referred to as template-assisted selective epitaxy (TASE).[211–213]

These systems are promising for creating large-scale device-ready junctions in a reproducible way like seen in Fig. 4(b). Moreover, the recent use of modulation (or remote) doping permits us to significantly decrease impurity induced scattering in such systems by coupling the core material with a doped one and designing the band structure to enhance the charge diffusion where desired [schematically depicted in the inset of Fig. 4(b)]. In this way, dopant induced scattering can be reduced by a separation of free carriers and physically doped layer, therefore increasing carrier densities and mobility.[12,165,170,214–219] The integration of such a doping technique into NW arrays can be a strong advantage not only for the material quality but also in terms of reproducibility. In fact, such a strategy allows us to decouple the optimization of crystal quality and the control over the electrical properties, with a great simplification of the growth process. Unfortunately, not all the architectures are compatible with remote doping, and its implementation in each particular device should be carefully evaluated.

V. DEVICES AND RELATED CHALLENGES

The achievement of commercially available NW devices requires innovative engineering. Besides the challenges concerning growth, characterization, and large area production discussed in Secs. II–IV, several application-specific obstacles also come into play. Indeed, the trade-off between material properties and the device requirements is critical for any kind of semiconductor device, independently of the scale of the active region. However, the significant impact of surface phenomena at the nanoscale makes nanowires unique systems, and therefore, specific device-related challenges have to be faced to achieve high performance. In this section, we will first focus on one very common element in nanowire devices: the electrical junctions. The design and fabrication of a nanoscale junction are strongly influenced by the material doping, and they have a strong impact on the device functionality. We will detail the critical aspects of an electrical nanowire junction, highlighting the issues that may arise due to limitations in controlling the doping concentration in interfaces and reduced volumes. Then, we will point out additional nanowire properties and phenomena, which are related to doping. Although they may appear negligible, they actually play a crucial role in improving the performance and figure of merit of the final device. Keeping in mind this purpose, we discuss the most common strategies to optimize the doping-related aspects of the design of nanowire-based devices.

A. Electrical junction in nanowire devices

All the electronic and opto-electronic devices respond to electrical and optical input by means of current rectification to manage their input or output signals. In a majority of cases, semiconductor technologies make use of electrical junctions as rectifying elements. In this context, III–V NW-based devices also need an electrical junction such as a nanoscale p-n (or p-i-n) junction. Only in a few applications, current rectification is achieved by exploiting other elements: examples

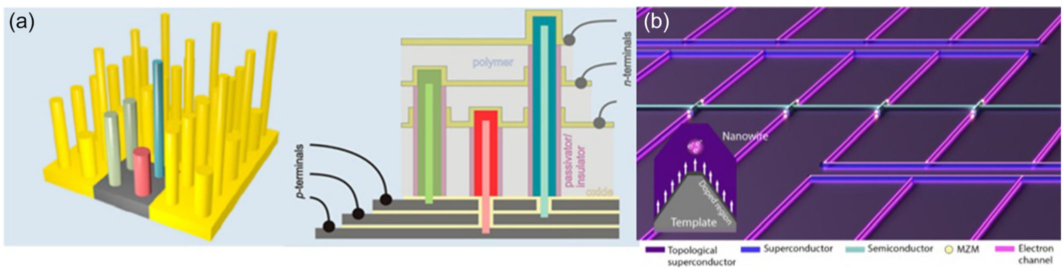

FIG. 4. NW based future device scheme. (a) Schematic illustration of the triple junction NW array on a Si substrate. Each unit cell contains high, low, and two medium bandgap nanowires (the higher the bandgap value, the higher the nanowires. Adapted with permission from Dorodnyy *et al.*, ACS Photonics 2, 1284 (2015). Copyright 2015 American Chemical Society). (b) Horizontal NW networks for Majorana zero mode (MZM) topological quantum computing inspired by Karzig *et al.*[201]

Published under license by AIP Publishing

are Schottky contacts in III–N NW piezoelectric generators[220,221] and hetero-barrier induced local electric fields in UV-photodetectors.[222–224] When designing an electrical junction in III–V nanowires, two architectures are available: axial and radial junctions. In fact, due to the 3D geometry of NWs, the electrical junctions can be embedded in NWs along their longitudinal[179,225,226] and along the radial direction.[80,173,227,228] The latter case is often referred to as core-shell junction since one semi-junction is fully wrapped into the other one. The debate on the pros and the cons of these two architectures is still ongoing, and no clear advantage of one over the other has still emerged.[229,230] In some applications, the junction design has a very high impact on the functionality of the device. For instance, the performance of nanowire solar cells containing an axial junction tends to be higher than their core/shell counterpart, although theoretically it should be the opposite due to the effect of surface recombination.[94,173] On the contrary, the design of LEDs and transistors with radial junctions appears more promising,[231,232] as demonstrated by gate all-around (GAA) transistors that are slowly finding their way in the industry world.[233] Indeed, the material growth parameters reflect the desired axial or radial architecture.[234] Therefore, the quality and properties of the junction are intimately related to the mechanisms ruling dopant incorporation.

As an example, we can emphasize on nanowires and mention growth-related challenges inherent to the axial junction, such as tapering. Depending on the growth conditions, as the nanowire grows, its diameter may taper due to the radial VS growth contribution. It is believed that the nanowire diameter will decrease linearly along the length. However, to maintain a constant doping concentration, the needed concentration of impurities varies hyperbolically with the diameter [Fig. 5(a)]. This is the reason why tapering phenomena are very likely to lead to doping fluctuations along the nanowire.

A common phenomenon occurring in VLS NWs containing axial compositional and electrical junctions is the infamous reservoir effect. It is generally accepted that having a crystal or a liquid acting as a "secondary reservoir" is detrimental to the accuracy and reproducibility of the growth: ideally, one wants a complete control over the incoming flux of materials, and a reservoir effect can cause an inertia in switching materials or doping elements, as depicted in Fig. 5(b). This will lead to a lack of sharpness in heterostructures (when different alloys are involved) or in the doping profile (when switching from a dopant species to another), as shown in Fig. 5(a).

In addition, VLS does not guarantee a homogeneous distribution of dopants into the wire during the growth, which must be carefully evaluated. The overall effect of these issues is the loss of control over the dopant concentration and distribution within the wire,[109] with a direct impact on the band structure and on the junction parameters. The consequences of the reservoir effect on the electrical properties can range from a decrease in the electric field across the junction to the onset of compensation mechanisms and consequent shift of the junction interface, up to a completely faulty junction.[72,91] In other terms, a significant unbalance in the doping design can compromise the functionality of the device. This is why a large literature section is devoted to the analysis of the doping concentration and profiles and of the abruptness of the junction, both from the experimental[72,235,236] and theoretical[237,238] perspectives [Fig. 5(c)].

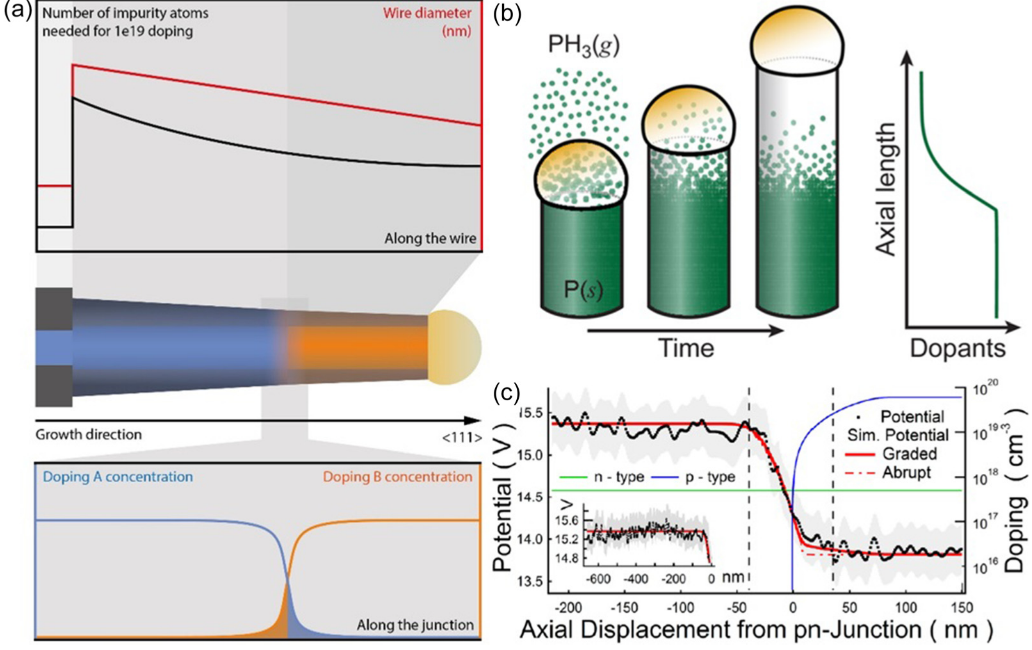

FIG. 5. Growth-related doping issues in nanowires. (a) Schematic representation of the influence of tapering and reservoir effects on the doping concentration (on top) and distribution (on the bottom). To maintain a constant doping concentration, the needed concentration of impurities varies hyperbolically with the diameter. (b) Schematic representation of the reservoir effect, which can cause an inertia in switching materials or doping elements. Adapted with permission from Christesen *et al.*, ACS Nano 8, 11790 (2014). Copyright 2014 American Chemical Society. (c) Investigation of the abruptness of an axial junction in GaAs NWs. Adapted with permission from Darbandi *et al.*, Nano Lett. 16, 3982 (2016). Copyright 2016 American Chemical Society.

Many approaches have been explored to mitigate this effect such as the use of solid catalysts[114] and vapor source pulsing.[239] Another strategy is the exploitation of VS growth mechanisms, thus eliminating the need for a liquid catalyst. However, as discussed in Sec. II, VLS-grown NWs have advantages with respect to VS ones, and therefore, a trade-off is usually considered.

The use of quick characterization techniques allows us to obtain rapid feedback and to improve the design in very short time. In this context, tools as EBIC and CL (described in Sec. III) are emerging, demonstrating how they can be used for both investigating and boosting devices.[173,179,231] In the field of NW solar cells, Otnes *et al.* shown exemplary junction parameter optimization.[73]

Iterative current–voltage (I–V) and EBIC measurements on single NWs and fully processed NW array devices enabled them to optimize the performance of InP NW array based solar cells. Their studies on interplay between growth parameters, processing conditions, and the solar cell power conversion efficiency (PCE) result in a more than sevenfold improvement in solar cell PCE (from 2% to 15.0%, certified by Fraunhofer ISE), achieving the highest reported value for a bottom-up synthesized InP nanowire solar cell. Similarly, several groups have used scanning probe techniques to identify limitations of NW devices and improve the design accordingly, obtaining an increase in performance.[49,240,241] In this context, these techniques can be used in a highly versatile way to face the challenges related to the band structure of III–V NWs.

Both tapering and reservoir effects may be influenced by local phenomena such as shadowing or substrate imperfections (which may influence the geometry of the droplet). This phenomenon may potentially lead to wire-to-wire inhomogeneity within the device. Also, in this case, the use of scanning probe techniques can be precious for identifying non-uniformity and correcting the design.[227,231]

Doping control in nanowires is fundamental also to determine reproducibly the electrical properties at the interface with the substrate. Indeed, a low dopant concentration close to the substrate can be a major problem for devices relying on nanostructured heterointerfaces. This is, for example, the case of nanostructured tandem solar cells.[242]

In such a system, two solar cells (one in the nanowire array and one in the substrate) are condensed in a two-terminal device. This scheme requires current matching between the two junctions through a tunnel diode, i.e., a junction between degenerate semiconductors.[243,244] Indeed, the most intuitive way to achieve the tunnel junction is to implant a high doping level in the substrate and to grow nanowires with very high doping stem. In this case, the ability to control the doping incorporation in the early stage of the growth is critical. Wallentin and coauthor reported the growth of the InP/GaAs tunnel diode, and Zeng and coauthors demonstrated the insertion of an InP/InGaP tunnel junction in the center of a bottom-up nanowire.[67,225] Sarwar and coauthors demonstrated the efficiency boost in UV LEDs made of III–N NWs with a tunnel junction placed 100 nm above the interface with the Si substrate.[245] To the best of our knowledge, no report on the tunnel diode at the heterointerface between bottom-up NWs and the substrate is still available.

Largely studied systems such as Si-doped GaAs NWs may be suited to investigate dopant incorporation at the substrate interface. Unfortunately, doping compensation limits the maximum achievable concentration down to roughly $5 \times 10^{18}\,\mathrm{cm}^{-3}$ (as previously mentioned), hindering the development of this type of tunnel diode on Si. Nevertheless, the only report on a nanostructured tandem solar cell relies on the coupling of these structures.[242] Deleterious effects can also arise when no junction is expected at the nanowire/substrate interface. Poor control over the local doping may result in an additional resistance (i.e., power losses in solar cells), which may be wrongly attributed to high defect density or band offset.[246,247]

B. Other doping related challenges

The functionality of electronic devices is highly affected by any doping variation since their figures of merit are directly related to the local and overall charge density, as well as the resulting internal electric fields. An example is given by the gate-all-around (GAA) FETs where an optimum source-drain doping concentration maximizes the ON current.[248] Where no optimization is achieved, the technologies cannot be fully exploited as in the case of III–V NWs for quantum transport application: on one side, high charge density is required to minimize the resistivity; on the other, the ionized impurities increase the electron scattering, hindering the required ballistic regime.[205] Facing and solving this kind of challenges—or taking advantage of them, whenever possible—is one of the keys to enable the fabrication of nonplanar electronic devices based on high mobility III–V NWs such as InAs and InSb.[106,249] One practical solution is the use of the so-called modulation (or remote) doping, already mentioned in Sec. IV. This approach has been used very effectively with InAs NWs. For example, in vertical intrinsic nanowires, epitaxially capped by the p-doped InP shell, the tunability of the hole concentration was demonstrated by changing the dopant concentration and thickness of shell.[250] More recently, this approach has been successfully applied to horizontal nanowires networks designed for quantum transport applications.[251] Due to the difficulty in improving the electrical properties at the nanoscale, iterative characterization gained a lot of attention as a fundamental part of the optimization process for nanowire-based devices.

Another relevant aspect for nanowires concerns the high surface-to-volume ratio and the strong impact of surface phenomena, which implies a consequence common to all nanostructured devices: the importance of the nanometric electrical connections. In addition to the possibility of having deleterious rectifying contacts, a low charge density localized close to the surface may induce a very high resistance into the system, i.e., a localized energy loss. Doping engineering must account also for this aspect, which involves the material coupling with metal contacts and the assessment of the electrical properties at the substrate interface.[252]

In high surface-to-volume structures such as nanowires, one should in addition consider the effect of surface phenomena such as the Fermi energy surface pinning on the nanostructures, as well as the dopant deactivation through the increase in their ionization energy.[117,122] In some cases, surface states can have a positive effect on the electrical properties. For example, intrinsic InAs NWs exhibit a high n-type conductivity due to the high density of donor-type surface states.[253] As a consequence, the electron accumulation layer at the surface may be beneficial for achieving low contact resistance; however, it also makes it challenging to achieve high p-type doping in InAs NWs due to compensation mechanisms. The opposite is happening in GaAs NWs where acceptor-like surface states are forming at the interface with the native oxide, pinning the Fermi energy close to the mid-gap

Published under license by AIP Publishing

value, creating a depleted surface layer, which limits the maximum doping concentration.[254,255] A wide research work has been done on the optimization of surface and interfaces, mainly through surface passivation.

By "passivation," the growth of few atomic layers of a dielectric[63] or semiconductor material[256] (ideally having an epitaxial relationship with the core semiconductor) aiming to reduce the densities of dangling bonds and charge trap at the surface is indicated. It is well established that passivation of the lateral areas can strongly enhance the carrier lifetime by reducing the non-radiative recombination rate. Moreover, by choosing the proper material coupling, also optical properties and internal stress can be tuned. For GaAs, the best passivation is achieved with AlGaAs,[118] which prevents the formation of native oxide and has a higher bandgap (so, it is suited to work as a window layer in solar cells). However, being very thin and hard to dope, these outer layers may form a highly resistive contact in actual devices. This is one of the main reason why several materials are still under research as a passivating or capping layer for a broad range of semiconductor nanowires.[257–259]

The variation of doping concentration may induce more complex phenomena in optoelectronic devices. For instance, photodetector figures of merit such as photoconductivity gain and photosensitivity are related to the dark current flowing in the device. Several investigations have been published on GaN NW photodetectors, showing how doping can impact the dark current and the collection of photogenerated carriers, together with its influence on optical properties (Burstein–Moss shift, compensation of eventual quantum Stark effects).[223,224,260,261] Moreover, it has been demonstrated that doping impacts the environmental sensitivity and the presence of persistent effects.[262] The case of LEDs is different as the optical properties of the active material have the highest influence on the figures of merit. Nevertheless, current injection and light extraction can be affected by the doping as in the case of the so-called "current crowding," which leads to a decrease in the IQE.[263,264]

VI. CONCLUSION AND OUTLOOK

In this review, the doping of bottom-up III–V NWs is discussed to highlight the impact of the scientific challenges on the integration of this technology in the industrial environment.

Indeed, the interplay between the kinetics of the growth and thermodynamic aspects affects the nanowire morphology in addition to the doping concentration and profile along different directions. In this regard, novel strategies have recently opened new possibilities to achieve superior control over the grown materials. On one side, the development of scanning characterization techniques and their implementation in the material design process can help in identifying and solving issues arising from a lack of doping control. On the other, the exploration of selective area growth epitaxy may ensure a higher reproducibility, therefore reducing the nanowire-to-nanowire performance scattering. Indeed, the research in this field will help to clarify the unexplored aspect of dopant incorporation and to achieve an increasingly higher control over doping of ordered III–V NWs in the near future. In addition, creative solutions are currently explored to speed up the development of NW-based devices, such as arrays made of morphologically different NWs and horizontal architectures. All these strategies can make the difference in transferring nanowire know-how from academic to industrial environments. Nevertheless, a large effort must still be devoted to facing challenges related to the fundamental physics occurring at the nanoscale to achieve high-performing devices. Some strategies are quite established in the field, such as the exploitation of VS growth to avoid reservoir effects and the use of passivation layers to reduce Fermi energy pinning. Other approaches have been applied to nanowires only recently, such as the use of modulation doping to improve the ballistic charge transport.

In conclusion, the recent advancements in the field of III–V NWs are oriented to improve the reproducibility and up-scalability of the fabrication methods through the control over doping. Accordingly, we believe that new insights and innovative findings will open a low dimensional material era based on the premise of multidisciplinary collaborative works of all the sectors involved in the design and optimization of commercial products.

AUTHORS' CONTRIBUTIONS

W.K. and L.G. contributed equally to this manuscript.

ACKNOWLEDGMENTS

W.K. and A.F.M. acknowledge H2020 funding through the project INDEED, L.G. and A.F.M. acknowledges SNSF through Project No. 200021_169908 and the NCCR QSIT. V.P. acknowledges the support by Piaget through the Scientific Award.

DATA AVAILABILITY

The data that support the findings of this study are available from the corresponding author upon reasonable request.

REFERENCES

[1]S. Rühle, "Tabulated values of the Shockley–Queisser limit for single junction solar cells," Sol. Energy **130**, 139 (2016).
[2]N. Waldron, C. Merckling, L. Teugels, P. Ong, S. A. U. Ibrahim, F. Sebaai, A. Pourghaderi, K. Barla, N. Collaert, and A. V.-Y. Thean, "InGaAs gate-all-around nanowire devices on 300 mm Si substrates," IEEE Electron Device Lett. **35**, 1097 (2014).
[3]D. Ren, X. Meng, Z. Rong, M. Cao, A. C. Farrell, S. Somasundaram, K. M. Azizur-Rahman, B. S. Williams, and D. L. Huffaker, "Uncooled photodetector at short-wavelength infrared using InAs nanowire photoabsorbers on InP with p–n heterojunctions," Nano Lett. **18**, 7901 (2018).
[4]J. Wallentin, N. Anttu, D. Asoli, M. Huffman, I. Aberg, M. H. Magnusson, G. Siefer, P. Fuss-Kailuweit, F. Dimroth, B. Witzigmann, H. Q. Xu, L. Samuelson, K. Deppert, and M. T. Borgstrom, "InP nanowire array solar cells achieving 13.8% efficiency by exceeding the ray optics limit," Science **339**, 1057 (2013).
[5]H. Sekiguchi, K. Kishino, and A. Kikuchi, "Emission color control from blue to red with nanocolumn diameter of InGaN/GaN nanocolumn arrays grown on same substrate," Appl. Phys. Lett. **96**, 231104 (2010).
[6]P. K. Sahoo, R. Janissen, M. P. Monteiro, A. Cavalli, D. M. Murillo, M. V. Merfa, C. L. Cesar, H. F. Carvalho, A. A. de Souza, E. P. A. M. Bakkers, and M. A. Cotta, "Nanowire arrays as cell force sensors to investigate adhesin-enhanced holdfast of single cell bacteria and biofilm stability," Nano Lett. **16**, 4656 (2016).
[7]H. Kim, A. C. Farrell, P. Senanayake, W.-J. Lee, and D. L. Huffaker, "Monolithically integrated InGaAs nanowires on 3D structured silicon-on-insulator as a new platform for full optical links," Nano Lett. **16**, 1833 (2016).
[8]A. C. Scofield, J. N. Shapiro, A. Lin, A. D. Williams, P.-S. Wong, B. L. Liang, and D. L. Huffaker, "Bottom-up photonic crystal cavities formed by patterned III–V nanopillars," Nano Lett. **11**, 2242 (2011).
[9]A. M. Munshi, D. L. Dheeraj, V. T. Fauske, D.-C. Kim, A. T. J. van Helvoort, B.-O. Fimland, and H. Weman, "Vertically aligned GaAs nanowires on

graphite and few-layer graphene: Generic model and epitaxial growth," Nano Lett. 12, 4570 (2012).
[10]P. K. Mohseni, A. Behnam, J. D. Wood, C. D. English, J. W. Lyding, E. Pop, and X. Li, "$In_xGa_{1-x}As$ nanowire growth on graphene: Van Der Waals epitaxy induced phase segregation," Nano Lett. 13, 1153 (2013).
[11]F. Schuster, S. Weiszer, M. Hetzl, A. Winnerl, J. A. Garrido, and M. Stutzmann, "Influence of substrate material, orientation, and surface termination on GaN nanowire growth," J. Appl. Phys. 116, 054301 (2014).
[12]K. Tomioka, M. Yoshimura, and T. Fukui, "A III–V nanowire channel on silicon for high-performance vertical transistors," Nature 488, 189 (2012).
[13]E. Barrigón, M. Heurlin, Z. Bi, B. Monemar, and L. Samuelson, "Synthesis and applications of III–V nanowires," Chemical Reviews 119, 9170 (2019).
[14]L. C. Chuang, M. Moewe, C. Chase, N. P. Kobayashi, C. Chang-Hasnain, and S. Crankshaw, "Critical diameter for III-V nanowires grown on lattice-mismatched substrates," Appl. Phys. Lett. 90, 043115 (2007).
[15]F. Glas, "Critical dimensions for the plastic relaxation of strained axial heterostructures in free-standing nanowires," Phys. Rev. B 74, 121302 (2006).
[16]M. T. Björk, B. J. Ohlsson, T. Sass, A. I. Persson, C. Thelander, M. H. Magnusson, K. Deppert, L. R. Wallenberg, and L. Samuelson, "One-dimensional steeplechase for electrons realized," Nano Lett. 2, 87 (2002).
[17]M. Hetzl, F. Schuster, A. Winnerl, S. Weiszer, and M. Stutzmann, "GaN nanowires on diamond," Mater. Sci. Semicond. Process. 48, 65 (2016).
[18]E. P. A. M. Bakkers, M. T. Borgström, and M. A. Verheijen, "Epitaxial growth of III-V nanowires on group IV substrates," MRS Bull. 32, 117 (2007).
[19]S. Conesa-Boj, E. Russo-Averchi, A. Dalmau-Mallorqui, J. Trevino, E. F. Pecora, C. Forestiere, A. Handin, M. Ek, L. Zweifel, L. R. Wallenberg, D. Rüffer, M. Heiss, D. Troadec, L. Dal Negro, P. Caroff, and A. Fontcuberta i Morral, "Vertical'III–V' V-shaped nanomembranes epitaxially grown on a patterned Si[001] substrate and their enhanced light scattering," ACS Nano 6, 10982 (2012).
[20]Z. Sun, O. Hazut, B.-C. Huang, Y.-P. Chiu, C.-S. Chang, R. Yerushalmi, L. J. Lauhon, and D. N. Seidman, "Dopant diffusion and activation in silicon nanowires fabricated by ex situ doping: A correlative study via atom-probe tomography and scanning tunneling spectroscopy," Nano Lett. 16, 4490 (2016).
[21]J. Wallentin and M. T. Borgström, "Doping of semiconductor nanowires," J. Mater. Res. 26, 2142 (2011).
[22]S. A. Dayeh, R. Chen, Y. G. Ro, and J. Sim, "Progress in doping semiconductor nanowires during growth," Mater. Sci. Semicond. Process. 62, 135 (2017).
[23]L. Güniat, S. Martí-Sánchez, O. Garcia, M. Boscardin, D. Vindice, N. Tappy, M. Friedl, W. Kim, M. Zamani, L. Francaviglia, A. Balgarkashi, J.-B. Leran, J. Arbiol, and A. Fontcuberta i Morral, "III–V integration on Si(100): Vertical nanospades," ACS Nano 13, 5833 (2019).
[24]C. Ronning, C. Borschel, S. Geburt, and R. Niepelt, "Ion beam doping of semiconductor nanowires," Mater. Sci. Eng.: R 70, 30 (2010).
[25]R. S. Wagner and W. C. Ellis, "Vapor-liquid-solid mechanism of single crystal growth," Appl. Phys. Lett. 4, 89 (1964).
[26]M. Albani, R. Bergamaschini, M. Salvalaglio, A. Voigt, L. Miglio, and F. Montalenti, "Competition between kinetics and thermodynamics during the growth of faceted crystal by phase field modeling," Physica Status Solidi (b) 256, 1800518 (2019).
[27]M. Albani, L. Ghisalberti, R. Bergamaschini, M. Friedl, M. Salvalaglio, A. Voigt, F. Montalenti, G. Tütüncüoglu, A. Fontcuberta i Morral, and L. Miglio, "Growth kinetics and morphological analysis of homoepitaxial GaAs fins by theory and experiment," Phys. Rev. Mater. 2, 093404 (2018).
[28]K. Ikejiri, J. Noborisaka, S. Hara, J. Motohisa, and T. Fukui, "Mechanism of catalyst-free growth of GaAs nanowires by selective area MOVPE," J. Cryst. Growth 298, 616 (2007).
[29]S. J. Gibson, J. P. Boulanger, and R. R. LaPierre, "Opportunities and pitfalls in patterned self-catalyzed GaAs nanowire growth on silicon," Semicond. Sci. Technol. 28, 105025 (2013).
[30]J. Vukajlovic-Plestina, W. Kim, V. G. Dubrovski, G. Tütüncüoğlu, M. Lagier, H. Potts, M. Friedl, and A. Fontcuberta i Morral, "Engineering the size distributions of ordered GaAs nanowires on silicon," Nano Lett. 17, 4101 (2017).
[31]J. Vukajlovic-Plestina, W. Kim, L. Ghisalberti, G. Varnavides, G. Tütüncuoglu, H. Potts, M. Friedl, L. Güniat, W. C. Carter, V. G. Dubrovskii, and A. Fontcuberta i Morral, "Fundamental aspects to localize self-catalyzed III-V nanowires on silicon," Nat. Commun. 10, 869 (2019).
[32]G. Otnes, M. Heurlin, M. Graczyk, J. Wallentin, D. Jacobsson, A. Berg, I. Maximov, and M. T. Borgström, "Strategies to obtain pattern fidelity in nanowire growth from large-area surfaces patterned using nanoimprint lithography," Nano Res. 9, 2852 (2016).
[33]H. Küpers, R. B. Lewis, A. Tahraoui, M. Matalla, O. Krüger, F. Bastiman, H. Riechert, and L. Geelhaar, "Diameter evolution of selective area grown Ga-assisted GaAs nanowires," Nano Res. 11, 2885 (2018).
[34]D. E. Perea, E. R. Hemesath, E. J. Schwalbach, J. L. Lensch-Falk, P. W. Voorhees, and L. J. Lauhon, "Direct measurement of dopant distribution in an individual vapour–liquid–solid nanowire," Nat. Nanotechnol. 4, 315 (2009).
[35]Q. Wu, N. Liu, Y. Zhang, W. Qian, X. Wang, and Z. Hu, "Tuning the field emission properties of AlN nanocones by doping," J. Mater. Chem. C 3, 1113 (2015).
[36]A. T. Connie, S. Zhao, S. Md. Sadaf, I. Shih, Z. Mi, X. Du, J. Lin, and H. Jiang, "Optical and electrical properties of Mg-doped AlN nanowires grown by molecular beam epitaxy," Applied Physics Letters 106, 213105 (2015).
[37]H. Hu, Z. Wu, W. Zhang, H. Li, R. Zhuo, D. Yan, J. Wang, and P. Yan, "Effect of Mg doping on growth and photoluminescence of AlN hexagonal nanorods," J. Alloys Compd. 624, 241 (2015).
[38]Y.-B. Tang, X.-H. Bo, J. Xu, Y.-L. Cao, Z.-H. Chen, H.-S. Song, C.-P. Liu, T.-F. Hung, W.-J. Zhang, H.-M. Cheng, I. Bello, S.-T. Lee, and C.-S. Lee, "Tunable P-type conductivity and transport properties of AlN nanowires via Mg doping," ACS Nano 5, 3591 (2011).
[39]Y. Y. Hui, J. Ye, R. Lortz, K. S. Teng, and S. P. Lau, "Magnetic properties of Mg-doped AlN zigzag nanowires," Phys. Status Solidi (a) 209, 1988 (2012).
[40]J. Liu, X.-M. Meng, Y. Jiang, C.-S. Lee, I. Bello, and S.-T. Lee, "Gallium nitride nanowires doped with silicon," Appl. Phys. Lett. 83, 4241 (2003).
[41]F. Schuster, A. Winnerl, S. Weiszer, M. Hetzl, J. A. Garrido, and M. Stutzmann, "Doped GaN nanowires on diamond: Structural properties and charge carrier distribution," J. Appl. Phys. 117, 044307 (2015).
[42]M. S. Son, S. I. Im, Y. S. Park, C. M. Park, T. W. Kang, and K.-H. Yoo, "Ultraviolet photodetector based on single GaN nanorod p–n junctions," Mater. Sci. Eng.: C 26, 886 (2006).
[43]W. Guo, M. Zhang, A. Banerjee, and P. Bhattacharya, "Catalyst-free InGaN/GaN nanowire light emitting diodes grown on (001) silicon by molecular beam epitaxy," Nano Lett. 10, 3355 (2010).
[44]F. Furtmayr, M. Vielemeyer, M. Stutzmann, A. Laufer, B. K. Meyer, and M. Eickhoff, "Optical properties of Si- and Mg-doped gallium nitride nanowires grown by plasma-assisted molecular beam epitaxy," J. Appl. Phys. 104, 074309 (2008).
[45]T. Frost, S. Jahangir, E. Stark, S. Deshpande, A. Hazari, C. Zhao, B. S. Ooi, and P. Bhattacharya, "Monolithic electrically injected nanowire array edge-emitting laser on (001) silicon," Nano Lett. 14, 4535 (2014).
[46]F. Qian, Y. Li, S. Gradečak, D. Wang, C. J. Barrelet, and C. M. Lieber, "Gallium nitride-based nanowire radial heterostructures for nanophotonics," Nano Lett. 4, 1975 (2004).
[47]N. Guan, X. Dai, A. Messanvi, H. Zhang, J. Yan, E. Gautier, C. Bougerol, F. H. Julien, C. Durand, J. Eymery, and M. Tchernycheva, "Flexible white light emitting diodes based on nitride nanowires and nanophosphors," ACS Photonics 3, 597 (2016).
[48]X. Dai, A. Messanvi, H. Zhang, C. Durand, J. Eymery, C. Bougerol, F. H. Julien, and M. Tchernycheva, "Flexible light-emitting diodes based on vertical nitride nanowires," Nano Lett. 15, 6958 (2015).
[49]P. Tchoulfian, F. Donatini, F. Levy, A. Dussaigne, P. Ferret, and J. Pernot, "Direct imaging of p−n junction in core−shell GaN wires," Nano Lett. 14, 3491 (2014).
[50]R. Koester, J.-S. Hwang, D. Salomon, X. Chen, C. Bougerol, J.-P. Barnes, D. L. S. Dang, L. Rigutti, A. de Luna Bugallo, G. Jacopin, M. Tchernycheva, C. Durand, and J. Eymery, "M-plane core–shell InGaN/GaN multiple-quantum-wells on GaN wires for electroluminescent devices," Nano Lett. 11, 4839 (2011).
[51]Z. Zhong, F. Qian, D. Wang, and C. M. Lieber, "Synthesis of p-type gallium nitride nanowires for electronic and photonic nanodevices," Nano Lett. 3, 343 (2003).

Published under license by AIP Publishing

[52]G. Cheng, A. Kolmakov, Y. Zhang, M. Moskovits, R. Munden, M. A. Reed, G. Wang, D. Moses, and J. Zhang, "Current rectification in a single GaN nanowire with a well-defined p–n junction," Appl. Phys. Lett. **83**, 1578 (2003).
[53]T. Richter, H. Lüth, T. Schäpers, R. Meijers, K. Jeganathan, S. Estévez Hernández, R. Calarco, and M. Marso, "Electrical transport properties of single undoped and N-type doped InN nanowires," Nanotechnology **20**, 405206 (2009).
[54]S. Zhao, S. Fathololoumi, K. H. Bevan, D. P. Liu, M. G. Kibria, Q. Li, G. T. Wang, H. Guo, and Z. Mi, "Tuning the surface charge properties of epitaxial InN nanowires," Nano Lett. **12**, 2877 (2012).
[55]R. Cuscó, N. Domènech-Amador, L. Artús, T. Gotschke, K. Jeganathan, T. Stoica, and R. Calarco, "Probing the electron density in undoped, Si-doped, and Mg-doped InN nanowires by means of Raman scattering," Appl. Phys. Lett. **97**, 221906 (2010).
[56]S. Zhao, B. H. Le, D. P. Liu, X. D. Liu, M. G. Kibria, T. Szkopek, H. Guo, and Z. Mi, "P-type InN nanowires," Nano Letters **13**, 5509 (2013).
[57]H. Song, A. Yang, R. Zhang, Y. Guo, H. Wei, G. Zheng, S. Yang, X. Liu, Q. Zhu, and Z. Wang, "Well-aligned Zn-doped InN nanorods grown by metal-organic chemical vapor deposition and the dopant distribution," Cryst. Growth Design **9**, 3292 (2009).
[58]S. Yazdi, A. Berg, M. T. Borgström, T. Kasama, M. Beleggia, L. Samuelson, and J. B. Wagner, "Doping GaP core-shell nanowire pn-junctions: A study by off-axis electron holography," Small **11**, 2687 (2015).
[59]Z.-G. Chen, L. Cheng, G. Q. (Max) Lu, and J. Zou, "Sulfur-doped gallium phosphide nanowires and their optoelectronic properties," Nanotechnology **21**, 375701 (2010).
[60]H. W. Seo, S. Y. Bae, J. Park, M. Kang, and S. Kim, "Nitrogen-doped gallium phosphide nanowires," Chem. Phys. Lett. **378**, 420 (2003).
[61]L. Rigutti, A. De Luna Bugallo, M. Tchernycheva, G. Jacopin, F. H. Julien, G. Cirlin, G. Patriarche, D. Lucot, L. Travers, and J.-C. Harmand, "Si incorporation in InP nanowires grown by Au-Assisted molecular beam epitaxy," J. Nanomater. **2009**, 1.
[62]H. Goto, K. Nosaki, K. Tomioka, S. Hara, K. Hiruma, J. Motohisa, and T. Fukui, "Growth of core–shell InP nanowires for photovoltaic application by selective-area metal organic vapor phase epitaxy," Appl. Phys. Express **2**, 035004 (2009).
[63]Z. Zhong, Z. Li, Q. Gao, Z. Li, K. Peng, L. Li, S. Mokkapati, K. Vora, J. Wu, G. Zhang, Z. Wang, L. Fu, H. H. Tan, and C. Jagadish, "Efficiency enhancement of axial junction InP single nanowire solar cells by dielectric coating," Nano Energy **28**, 106 (2016).
[64]Y. Cui, J. Wang, S. R. Plissard, A. Cavalli, T. T. T. Vu, R. P. J. van Veldhoven, L. Gao, M. Trainor, M. A. Verheijen, J. E. M. Haverkort, and E. P. A. M. Bakkers, "Efficiency enhancement of InP nanowire solar cells by surface cleaning," Nano Lett. **13**, 4113 (2013).
[65]E. D. Minot, F. Kelkensberg, M. van Kouwen, J. A. van Dam, L. P. Kouwenhoven, V. Zwiller, M. T. Borgström, O. Wunnicke, M. A. Verheijen, and E. P. A. M. Bakkers, "Single quantum dot nanowire LEDs," Nano Lett. **7**, 367 (2007).
[66]M. H. M. van Weert, A. Helman, W. van den Einden, R. E. Algra, M. A. Verheijen, M. T. Borgström, G. Immink, J. J. Kelly, L. P. Kouwenhoven, and E. P. A. M. Bakkers, "Zinc incorporation via the vapor−liquid−solid mechanism into InP nanowires," J. Am. Chem. Soc. **131**, 4578 (2009).
[67]J. Wallentin, J. M. Persson, J. B. Wagner, L. Samuelson, K. Deppert, and M. T. Borgström, "High-performance single nanowire tunnel diodes," Nano Lett. **10**, 974 (2010).
[68]X. Duan, Y. Huang, Y. Cui, J. Wang, and C. M. Lieber, "Indium phosphide nanowires as building blocks for nanoscale electronic and optoelectronic devices," Nature **409**, 66 (2001).
[69]M. H. M. van Weert, O. Wunnicke, A. L. Roest, T. J. Eijkemans, A. Yu Silov, J. E. M. Haverkort, G. W. 't Hooft, and E. P. A. M. Bakkers, "Large redshift in photoluminescence of p-doped InP nanowires induced by Fermi-level pinning," Appl. Phys. Lett. **88**, 043109 (2006).
[70]M. T. Borgström, E. Norberg, P. Wickert, H. A. Nilsson, J. Trägårdh, K. A. Dick, G. Statkute, P. Ramvall, K. Deppert, and L. Samuelson, "Precursor evaluation for in situ InP nanowire doping," Nanotechnology **19**, 445602 (2008).
[71]M. Heurlin, P. Wickert, S. Fält, M. T. Borgström, K. Deppert, L. Samuelson, and M. H. Magnusson, "Axial InP nanowire tandem junction grown on a silicon substrate," Nano Lett. **11**, 2028 (2011).
[72]V. Jain, A. Nowzari, J. Wallentin, M. T. Borgström, M. E. Messing, D. Asoli, M. Graczyk, B. Witzigmann, F. Capasso, L. Samuelson, and H. Pettersson, "Study of photocurrent generation in InP nanowire-based P+-i-N+ photodetectors," Nano Res. **7**, 544 (2014).
[73]G. Otnes, E. Barrigón, C. Sundvall, K. E. Svensson, M. Heurlin, G. Siefer, L. Samuelson, I. Åberg, and M. T. Borgström, "Understanding InP nanowire array solar cell performance by nanoprobe-enabled single nanowire measurements," Nano Lett. **18**, 3038 (2018).
[74]H. Pettersson, I. Zubritskaya, N. T. Nghia, J. Wallentin, M. T. Borgström, K. Storm, L. Landin, P. Wickert, F. Capasso, and L. Samuelson, "Electrical and optical properties of InP nanowire ensemble p^+–i–n^+ photodetectors," Nanotechnology **23**, 135201 (2012).
[75]S. De Franceschi, J. A. van Dam, E. P. A. M. Bakkers, L. F. Feiner, L. Gurevich, and L. P. Kouwenhoven, "Single-electron tunneling in InP nanowires," Appl. Phys. Lett. **83**, 344 (2003).
[76]C. Liu, L. Dai, L. P. You, W. J. Xu, and G. G. Qin, "Blueshift of electroluminescence from single N-InP nanowire/p-Si heterojunctions due to the Burstein–Moss effect," Nanotechnology **19**, 465203 (2008).
[77]J. Wallentin, M. Ek, L. R. Wallenberg, L. Samuelson, K. Deppert, and M. T. Borgström, "Changes in contact angle of seed particle correlated with increased zincblende formation in doped InP nanowires," Nano Lett. **10**, 4807 (2010).
[78]R. E. Algra, M. A. Verheijen, M. T. Borgström, L.-F. Feiner, G. Immink, W. J. P. van Enckevort, E. Vlieg, and E. P. A. M. Bakkers, "Twinning superlattices in indium phosphide nanowires," Nature **456**, 369 (2008).
[79]H. G. Lee, H. C. Jeon, T. W. Kang, and T. W. Kim, "Gallium arsenide crystalline nanorods grown by molecular-beam epitaxy," Appl. Phys. Lett. **78**, 3319 (2001).
[80]C. Colombo, M. Heiβ, M. Grätzel, and A. Fontcuberta i Morral, "Gallium arsenide p-i-n radial structures for photovoltaic applications," Appl. Phys. Lett. **94**, 173108 (2009).
[81]M. Hilse, M. Ramsteiner, S. Breuer, L. Geelhaar, and H. Riechert, "Incorporation of the dopants Si and Be into GaAs nanowires," Appl. Phys. Lett. **96**, 193104 (2010).
[82]K. Tomioka, J. Motohisa, S. Hara, K. Hiruma, and T. Fukui, "GaAs/AlGaAs core multishell nanowire-based light-emitting diodes on Si," Nano Lett. **10**, 1639 (2010).
[83]K. Haraguchi, T. Katsuyama, K. Hiruma, and K. Ogawa, "GaAs p-n junction formed in quantum wire crystals," Appl. Phys. Lett. **60**, 745 (1992).
[84]K. Sladek, V. Klinger, J. Wensorra, M. Akabori, H. Hardtdegen, and D. Grützmacher, "MOVPE of N-doped GaAs and modulation doped GaAs/AlGaAs nanowires," J. Cryst. Growth **312**, 635 (2010).
[85]G. Mariani, P.-S. Wong, A. M. Katzenmeyer, F. Léonard, J. Shapiro, and D. L. Huffaker, "Patterned radial GaAs nanopillar solar cells," Nano Lett. **11**, 2490 (2011).
[86]B. Ketterer, E. Mikheev, E. Uccelli, and A. Fontcuberta i Morral, "Compensation mechanism in silicon-doped gallium arsenide nanowires," Appl. Phys. Lett. **97**, 223103 (2010).
[87]J. Dufouleur, C. Colombo, T. Garma, B. Ketterer, E. Uccelli, M. Nicotra, and A. Fontcuberta i Morral, "p-doping mechanisms in catalyst-free gallium arsenide nanowires," Nano Lett. **10**, 1734 (2010).
[88]G. Mariani, A. C. Scofield, C.-H. Hung, and D. L. Huffaker, "GaAs nanopillar-array solar cells employing in situ surface passivation," Nat. Commun. **4**, 1497 (2013).
[89]T. Hakkarainen, M. Rizzo Piton, E. M. Fiordaliso, E. D. Leshchenko, S. Koelling, J. Bettini, H. Vinicius Avanço Galeti, E. Koivusalo, Y. G. Gobato, A. de Giovanni Rodrigues, D. Lupo, P. M. Koenraad, E. R. Leite, V. G. Dubrovskii, and M. Guina, "Te incorporation and activation as n-type dopant in self-catalyzed GaAs nanowires," Phys. Rev. Mater. **3**, 086001 (2019).
[90]J. Caram, C. Sandoval, M. Tirado, D. Comedi, J. Czaban, D. A. Thompson, and R. R. LaPierre, "Electrical characteristics of core–shell p–n GaAs nanowire structures with Te as the n-dopant," Nanotechnology **21**, 134007 (2010).
[91]J. A. Czaban, D. A. Thompson, and R. R. LaPierre, "GaAs core−shell nanowires for photovoltaic applications," Nano Lett. **9**, 148 (2009).
[92]A. Lysov, M. Offer, C. Gutsche, I. Regolin, S. Topaloglu, M. Geller, W. Prost, and F.-J. Tegude, "Optical properties of heavily doped GaAs nanowires and electroluminescent nanowire structures," Nanotechnology **22**, 085702 (2011).

Published under license by AIP Publishing

[93] I. Regolin, C. Gutsche, A. Lysov, K. Blekker, Z.-A. Li, M. Spasova, W. Prost, and F.-J. Tegude, "Axial pn-junctions formed by MOVPE using DEZn and TESn in vapor–liquid–solid grown GaAs nanowires," J. Cryst. Growth **315**, 143 (2011).
[94] I. Aberg, G. Vescovi, D. Asoli, U. Naseem, J. P. Gilboy, C. Sundvall, A. Dahlgren, K. E. Svensson, N. Anttu, M. T. Bjork, and L. Samuelson, "A GaAs nanowire array solar cell with 15.3% efficiency at 1 sun," IEEE J. Photovoltaics **6**, 185 (2016).
[95] A. Casadei, P. Krogstrup, M. Heiss, J. A. Röhr, C. Colombo, T. Ruelle, S. Upadhyay, C. B. Sørensen, J. Nygård, and A. Fontcuberta i Morral, "Doping incorporation paths in catalyst-free Be-doped GaAs nanowires," Appl. Phys. Lett. **102**, 013117 (2013).
[96] G. E. Cirlin, A. D. Bouravleuv, I. P. Soshnikov, Yu. B. Samsonenko, V. G. Dubrovskii, E. M. Arakcheeva, E. M. Tanklevskaya, and P. Werner, "Photovoltaic properties of p-doped gaas nanowire arrays grown on n-type GaAs(111)B substrate," Nanoscale Res. Lett. **5**, 360 (2010).
[97] C. Gutsche, I. Regolin, K. Blekker, A. Lysov, W. Prost, and F. J. Tegude, "Controllable p-type doping of GaAs nanowires during vapor-liquid-solid growth," J. Appl. Phys. **105**, 024305 (2009).
[98] H. Gamo and K. Tomioka, "Selective-area growth of pulse-doped InAs nanowires on Si and vertical transistor application," J. Cryst. Growth **500**, 58 (2018).
[99] G. Astromskas, K. Storm, O. Karlström, P. Caroff, M. Borgström, and L.-E. Wernersson, "Doping incorporation in InAs nanowires characterized by capacitance measurements," J. Appl. Phys. **108**, 054306 (2010).
[100] C. Thelander, K. A. Dick, M. T. Borgström, L. E. Fröberg, P. Caroff, H. A. Nilsson, and L. Samuelson, "The electrical and structural properties of n-type InAs nanowires grown from metal–organic precursors," Nanotechnology **21**, 205703 (2010).
[101] S. Wirths, K. Weis, A. Winden, K. Sladek, C. Volk, S. Alagha, T. E. Weirich, M. von der Ahe, H. Hardtdegen, H. Lüth, N. Demarina, D. Grützmacher, and Th. Schäpers, "Effect of Si-doping on InAs nanowire transport and morphology," J. Appl. Phys. **110**, 053709 (2011).
[102] B. S. Sørensen, M. Aagesen, C. B. Sørensen, P. E. Lindelof, K. L. Martinez, and J. Nygård, "Ambipolar transistor behavior in p-doped InAs nanowires grown by molecular beam epitaxy," Appl. Phys. Lett. **92**, 012119 (2008).
[103] M. D. Thompson, A. Alhodaib, A. P. Craig, A. Robson, A. Aziz, A. Krier, J. Svensson, L.-E. Wernersson, A. M. Sanchez, and A. R. J. Marshall, "Low leakage-current InAsSb nanowire photodetectors on silicon," Nano Lett. **16**, 182 (2016).
[104] I. Khytruk, A. Druzhinin, I. Ostrovskii, Y. Khoverko, N. Liakh-Kaguy, and K. Rogacki, "Properties of doped GaSb whiskers at low temperatures," Nanoscale Res. Lett. **12**, 156 (2017).
[105] B. M. Borg, M. Ek, B. Ganjipour, A. W. Dey, K. A. Dick, L.-E. Wernersson, and C. Thelander, "Influence of doping on the electronic transport in GaSb/InAs(Sb) nanowire tunnel devices," Appl. Phys. Lett. **101**, 043508 (2012).
[106] Z. Yang, N. Han, F. Wang, H.-Y. Cheung, X. Shi, S. Yip, T. Hung, M. H. Lee, C.-Y. Wong, and J. C. Ho, "Carbon doping of InSb nanowires for high-performance p-channel field-effect-transistors," Nanoscale **5**, 9671 (2013).
[107] S. C. Erwin, L. Zu, M. I. Haftel, A. L. Efros, T. A. Kennedy, and D. J. Norris, "Doping semiconductor nanocrystals," Nature **436**, 91 (2005).
[108] M. T. Borgström, J. Wallentin, J. Trägårdh, P. Ramvall, M. Ek, L. R. Wallenberg, L. Samuelson, and K. Deppert, "In situ etching for total control over axial and radial nanowire growth," Nano Research **3**, 264 (2010).
[109] J. G. Connell, K. Yoon, D. E. Perea, E. J. Schwalbach, P. W. Voorhees, and L. J. Lauhon, "Identification of an intrinsic source of doping inhomogeneity in vapor–liquid–solid-grown nanowires," Nano Lett. **13**, 199 (2013).
[110] M. H. T. Dastjerdi, E. M. Fiordaliso, E. D. Leshchenko, A. Akhtari-Zavareh, T. Kasama, M. Aagesen, V. G. Dubrovskii, and R. R. LaPierre, "Three-fold symmetric doping mechanism in GaAs nanowires," Nano Lett. **17**, 5875 (2017).
[111] Y. Zhang, Z. Sun, A. M. Sanchez, M. Ramsteiner, M. Aagesen, J. Wu, D. Kim, P. Jurczak, S. Huo, L. J. Lauhon, and H. Liu, "Doping of self-catalyzed nanowires under the influence of droplets," Nano Lett. **18**, 81 (2018).
[112] H. Hijazi, G. Monier, E. Gil, A. Trassoudaine, C. Bougerol, C. Leroux, D. Castellucci, C. Robert-Goumet, P. E. Hoggan, Y. André, N. Isik Goktas, R. R. LaPierre, and V. G. Dubrovskii, "Si doping of vapor–liquid–solid GaAs nanowires: N-type or p-type?," Nano Letters **19**, 4498 (2019).
[113] V. G. Dubrovskii and H. Hijazi, "Effect of arsenic depletion on the silicon doping of vapor–liquid–solid GaAs nanowires," Phys. Status Solidi (RRL) **14**, 2000129 (2020).
[114] C.-Y. Wen, M. C. Reuter, J. Bruley, J. Tersoff, S. Kodambaka, E. A. Stach, and F. M. Ross, "Formation of compositionally abrupt axial heterojunctions in silicon-germanium nanowires," Science **326**, 1247 (2009).
[115] J. E. Allen, E. R. Hemesath, and L. J. Lauhon, "Scanning photocurrent microscopy analysis of Si nanowire field-effect transistors fabricated by surface etching of the channel," Nano Lett. **9**, 1903 (2009).
[116] E. Koren, J. K. Hyun, U. Givan, E. R. Hemesath, L. J. Lauhon, and Y. Rosenwaks, "Obtaining uniform dopant distributions in VLS-grown Si nanowires," Nano Lett. **11**, 183 (2011).
[117] M. T. Björk, H. Schmid, J. Knoch, H. Riel, and W. Riess, "Donor deactivation in silicon nanostructures," Nat. Nanotechnol. **4**, 103 (2009).
[118] C.-C. Chang, C.-Y. Chi, M. Yao, N. Huang, C.-C. Chen, J. Theiss, A. W. Bushmaker, S. LaLumondiere, T.-W. Yeh, M. L. Povinelli, C. Zhou, P. D. Dapkus, and S. B. Cronin, "Electrical and optical characterization of surface passivation in GaAs nanowires," Nano Lett. **12**, 4484 (2012).
[119] C.-Y. Wu and J.-F. Chen, "Doping and temperature dependences of minority-carrier diffusion length and lifetime deduced from the spectral response measurements of p-n junction solar cells," Solid-State Electron. **25**, 679 (1982).
[120] C. C. Wu, K. C. Lin, S. H. Chan, M. S. Feng, and C. Y. Chang, "Doping of InGaP epitaxial layers grown by low pressure metal-organic chemical vapor deposition," Mater. Sci. Eng.: B **19**, 234 (1993).
[121] D. D. Perovic, M. R. Castell, A. Howie, C. Lavoie, T. Tiedje, and J. S. W. Cole, "Field-emission SEM imaging of compositional and doping layer semiconductor superlattices," Ultramicroscopy **58**, 104 (1995).
[122] R. Calarco, M. Marso, T. Richter, A. I. Aykanat, R. Meijers, A. v.d. Hart, T. Stoica, and H. Lüth, "Size-dependent photoconductivity in MBE-grown GaN-nanowires," Nano Lett. **5**, 981 (2005).
[123] C. Gutsche, R. Niepelt, M. Gnauck, A. Lysov, W. Prost, C. Ronning, and F.-J. Tegude, "Direct determination of minority carrier diffusion lengths at axial GaAs nanowire p–n junctions," Nano Lett. **12**, 1453 (2012).
[124] N. I. Goktas, E. M. Fiordaliso, and R. R. LaPierre, "Doping assessment in GaAs nanowires," Nanotechnology **29**, 234001 (2018).
[125] M. A. Seyedi, M. Yao, J. O'Brien, S. Y. Wang, and P. D. Dapkus, "Large area, low capacitance, GaAs nanowire photodetector with a transparent Schottky collecting junction," Appl. Phys. Lett. **103**, 251109 (2013).
[126] P. Senanayake, A. Lin, G. Mariani, J. Shapiro, C. Tu, A. C. Scofield, P.-S. Wong, B. Liang, and D. L. Huffaker, "Photoconductive gain in patterned nanopillar photodetector arrays," Appl. Phys. Lett. **97**, 203108 (2010).
[127] D. Mikulik, M. Ricci, G. Tutuncuoglu, F. Matteini, J. Vukajlovic, N. Vulic, E. Alarcon-Llado, and A. Fontcuberta i Morral, "Conductive-probe atomic force microscopy as a characterization tool for nanowire-based solar cells," Nano Energy **41**, 566 (2017).
[128] D. E. Newbury and N. W. M. Ritchie, "Is scanning electron microscopy/energy dispersive x-ray spectrometry (SEM/EDS) quantitative?: Quantitative SEM/EDS analysis," Scanning **35**, 141 (2013).
[129] P. V. Radovanovic, K. G. Stamplecoskie, and B. G. Pautler, "Dopant ion concentration dependence of growth and faceting of manganese-doped GaN nanowires," J. Am. Chem. Soc. **129**, 10980 (2007).
[130] J. Veerbeek, L. Ye, W. Vijselaar, T. Kudernac, W. G. van der Wiel, and J. Huskens, "Highly doped silicon nanowires by monolayer doping," Nanoscale **9**, 2836 (2017).
[131] A. Smyrnakis, P. Dimitrakis, and E. Gogolides, "Plasma-etched, silicon nanowire, radial junction photovoltaic device," J. Phys. D **51**, 455101 (2018).
[132] A. Klump, C. Zhou, F. A. Stevie, R. Collazo, and Z. Sitar, "Improvement in detection limit for time-of-flight SIMS analysis of dopants in GaN structures," J. Vac. Sci. Technol., B **36**, 03F102 (2018).
[133] J. A. Whitby, F. Östlund, P. Horvath, M. Gabureac, J. L. Riesterer, I. Utke, M. Hohl, L. Sedláček, J. Jiruše, V. Friedli, M. Bechelany, and J. Michler, "High spatial resolution time-of-flight secondary ion mass spectrometry for the masses: A novel orthogonal ToF FIB-SIMS instrument with in situ AFM," Adv. Mater. Sci. Eng. **2012**, 1.
[134] W. Vandervorst, C. Fleischmann, J. Bogdanowicz, A. Franquet, U. Celano, K. Paredis, and A. Budrevich, "Dopant, composition and carrier profiling for 3D structures," Mater. Sci. Semicond. Process. **62**, 31 (2017).

Published under license by AIP Publishing

[135]A. C. E. Chia, N. Dhindsa, J. P. Boulanger, B. A. Wood, S. S. Saini, and R. R. LaPierre, "Nanowire dopant measurement using secondary ion mass spectrometry," J. Appl. Phys. **118**, 114306 (2015).
[136]A. C. E. Chia, J. P. Boulanger, and R. R. LaPierre, "Unlocking doping and compositional profiles of nanowire ensembles using SIMS," Nanotechnology **24**, 045701 (2013).
[137]B. Gault, M. P. Moody, F. De Geuser, A. La Fontaine, L. T. Stephenson, D. Haley, and S. P. Ringer, "Spatial resolution in atom probe tomography," Microsc. Microanal. **16**, 99 (2010).
[138]D. N. Seidman, "Three-dimensional atom-probe tomography: Advances and applications," Annu. Rev. Mater. Res. **37**, 127 (2007).
[139]L. Mancini, D. Hernández-Maldonado, W. Lefebvre, J. Houard, I. Blum, F. Vurpillot, J. Eymery, C. Durand, M. Tchernycheva, and L. Rigutti, "Multi-microscopy study of the influence of stacking faults and three-dimensional in distribution on the optical properties of m-plane InGaN quantum wells grown on microwire sidewalls," Appl. Phys. Lett. **108**, 042102 (2016).
[140]L. Mancini, Y. Fontana, S. Conesa-Boj, I. Blum, F. Vurpillot, L. Francaviglia, E. Russo-Averchi, M. Heiss, J. Arbiol, A. F. i Morral, and L. Rigutti, "Three-dimensional nanoscale study of Al segregation and quantum dot formation in GaAs/AlGaAs core-shell nanowires," Appl. Phys. Lett. **105**, 243106 (2014).
[141]X. Ren, J. R. Riley, D. D. Koleske, and L. J. Lauhon, "Correlated high-resolution x-ray diffraction, photoluminescence, and atom probe tomography analysis of continuous and discontinuous $In_xGa_{1-x}N$ quantum wells," Appl. Phys. Lett. **107**, 022107 (2015).
[142]R. Agrawal, R. A. Bernal, D. Isheim, and H. D. Espinosa, "Characterizing atomic composition and dopant distribution in wide band gap semiconductor nanowires using laser-assisted atom probe tomography," J. Phys. Chem. C **115**, 17688 (2011).
[143]S. Du, T. Burgess, B. Gault, Q. Gao, P. Bao, L. Li, X. Cui, W. Kong Yeoh, H. Liu, L. Yao, A. V. Ceguerra, H. Hoe Tan, C. Jagadish, S. P. Ringer, and R. Zheng, "Quantitative dopant distributions in GaAs nanowires using atom probe tomography," Ultramicroscopy **132**, 186 (2013).
[144]J. Becker, M. O. Hill, M. Sonner, J. Treu, M. Döblinger, A. Hirler, H. Riedl, J. J. Finley, L. Lauhon, and G. Koblmüller, "Correlated chemical and electrically active dopant analysis in catalyst-free Si-doped InAs nanowires," ACS Nano **12**, 1603 (2018).
[145]E. Stern, G. Cheng, J. F. Klemic, E. Broomfield, D. Turner-Evans, C. Li, C. Zhou, and M. A. Reed, "Methods for fabricating ohmic contacts to nanowires and nanotubes," J. Vac. Sci. Technol., B: Microelectron. Nanometer Struct.—Process., Meas., Phenom. **24**, 231 (2006).
[146]P. Blanc, M. Heiss, C. Colombo, A. D. Mallorquì, T. S. Safaei, P. Krogstrup, J. Nygård, and A. F. i Morral, "Electrical contacts to single nanowires: A scalable method allowing multiple devices on a chip. Application to a single nanowire radial p-i-n junction," Int. J. Nanotechnol. **10**, 419 (2013).
[147]X. Zeng, R. T. Mourão, G. Otnes, O. Hultin, V. Dagytė, M. Heurlin, and M. T. Borgström, "Electrical and optical evaluation of n-type doping in $In_xGa_{(1-x)}P$ nanowires," Nanotechnology **29**, 255701 (2018).
[148]K. Storm, F. Halvardsson, M. Heurlin, D. Lindgren, A. Gustafsson, P. M. Wu, B. Monemar, and L. Samuelson, "Spatially resolved hall effect measurement in a single semiconductor nanowire," Nat. Nanotechnol. **7**, 718 (2012).
[149]E. Stern, G. Cheng, M. P. Young, and M. A. Reed, "Specific contact resistivity of nanowire devices," Appl. Phys. Lett. **88**, 053106 (2006).
[150]A. V. Thathachary, N. Agrawal, L. Liu, and S. Datta, "Electron transport in multigate $In_xGa_{1-x}As$ nanowire FETs: From diffusive to ballistic regimes at room temperature," Nano Lett. **14**, 626 (2014).
[151]S. M. Sze and J. C. Irvin, "Resistivity, mobility and impurity levels in GaAs, Ge, and Si at 300 K," Solid-State Electron. **11**, 599 (1968).
[152]N. Clément, K. Nishiguchi, A. Fujiwara, and D. Vuillaume, "Evaluation of a gate capacitance in the sub-AF range for a chemical field-effect transistor with a Si nanowire channel," IEEE Trans. Nanotechnol. **10**, 1172 (2011).
[153]R. Tu, L. Zhang, Y. Nishi, and H. Dai, "Measuring the capacitance of individual semiconductor nanowires for carrier mobility assessment," Nano Lett. **7**, 1561 (2007).
[154]O. Hultin, G. Otnes, M. T. Borgström, M. Björk, L. Samuelson, and K. Storm, "Comparing Hall effect and field effect measurements on the same single nanowire," Nano Lett. **16**, 205 (2016).
[155]V. Schmidt, P. F. J. Mensch, S. F. Karg, B. Gotsmann, P. Das Kanungo, H. Schmid, and H. Riel, "Using the Seebeck coefficient to determine charge carrier concentration, mobility, and relaxation time in InAs nanowires," Appl. Phys. Lett. **104**, 012113 (2014).
[156]M. J. Deen and F. Pascal, "Electrical characterization of semiconductor materials and devices," in *Springer Handbook of Electronic and Photonic Materials*, edited by S. Kasap and P. Capper (Springer International Publishing, Cham, 2017), pp. 1–1.
[157]S. K. Ojha, P. K. Kasanaboina, C. L. Reynolds, T. A. Rawdanowicz, Y. Liu, R. M. White, and S. Iyer, "Incorporation of Be dopant in GaAs core and core–shell nanowires by molecular beam epitaxy," J. Vac. Sci. Technol., B **34**, 02L114 (2016).
[158]M. S. Mohajerani, S. Khachadorian, T. Schimpke, C. Nenstiel, J. Hartmann, J. Ledig, A. Avramescu, M. Strassburg, A. Hoffmann, and A. Waag, "Evaluation of local free carrier concentrations in individual heavily-doped GaN:Si micro-rods by micro-Raman spectroscopy," Appl. Phys. Lett. **108**, 091112 (2016).
[159]E. Dimakis, M. Ramsteiner, A. Tahraoui, H. Riechert, and L. Geelhaar, "Shell-doping of GaAs nanowires with Si for n-type conductivity," Nano Res. **5**, 796 (2012).
[160]S. C. Jain, J. M. McGregor, and D. J. Roulston, "Band-gap narrowing in novel III-V semiconductors," J. Appl. Phys. **68**, 3747 (1990).
[161]M. K. Hudait, P. Modak, and S. B. Krupanidhi, "Si incorporation and Burstein–Moss shift in n-type GaAs," Mater. Sci. Eng., B **60**(1), 1 (1999).
[162]S. N. Svitasheva and A. M. Gilinsky, "Influence of doping level on shift of the absorption edge of gallium nitride films (Burstein-Moss effect)," Appl. Surf. Sci. **281**, 109 (2013).
[163]S. Arab, M. Yao, C. Zhou, P. D. Dapkus, and S. B. Cronin, "Doping concentration dependence of the photoluminescence spectra of n-type GaAs nanowires," Appl. Phys. Lett. **108**, 182106 (2016).
[164]J. A. Alanis, M. Lysevych, T. Burgess, D. Saxena, S. Mokkapati, S. Skalsky, X. Tang, P. Mitchell, A. S. Walton, H. H. Tan, C. Jagadish, and P. Parkinson, "Optical study of p-doping in GaAs nanowires for low-threshold and high-yield lasing," Nano Lett. **19**, 362 (2019).
[165]J. L. Boland, S. Conesa-Boj, P. Parkinson, G. Tütüncüoglu, F. Matteini, D. Rüffer, A. Casadei, F. Amaduzzi, F. Jabeen, C. L. Davies, H. J. Joyce, L. M. Herz, A. Fontcuberta i Morral, and M. B. Johnston, "Modulation doping of GaAs/AlGaAs core–shell nanowires with effective defect passivation and high electron mobility," Nano Lett. **15**, 1336 (2015).
[166]H. J. Joyce, J. L. Boland, C. L. Davies, S. A. Baig, and M. B. Johnston, "A review of the electrical properties of semiconductor nanowires: Insights gained from terahertz conductivity spectroscopy," Semicond. Sci. Technol. **31**, 103003 (2016).
[167]J. L. Boland, A. Casadei, G. Tütüncüoglu, F. Matteini, C. L. Davies, F. Jabeen, H. J. Joyce, L. M. Herz, A. Fontcuberta i Morral, and M. B. Johnston, "Increased photoconductivity lifetime in GaAs nanowires by controlled n-type and p-type doping," ACS Nano **10**, 4219 (2016).
[168]H. J. Joyce, C. J. Docherty, Q. Gao, H. H. Tan, C. Jagadish, J. Lloyd-Hughes, L. M. Herz, and M. B. Johnston, "Electronic properties of GaAs, InAs and InP nanowires studied by terahertz spectroscopy," Nanotechnology **24**, 214006 (2013).
[169]J. L. Boland, F. Amaduzzi, S. Sterzl, H. Potts, L. M. Herz, A. Fontcuberta i Morral, and M. B. Johnston, "High electron mobility and insights into temperature-dependent scattering mechanisms in InAsSb nanowires," Nano Lett. **18**, 3703 (2018).
[170]J. L. Boland, G. Tütüncüoglu, J. Q. Gong, S. Conesa-Boj, C. L. Davies, L. M. Herz, A. Fontcuberta i Morral, and M. B. Johnston, "Towards higher electron mobility in modulation doped GaAs/AlGaAs core shell nanowires," Nanoscale **9**, 7839 (2017).
[171]H. J. Joyce, P. Parkinson, N. Jiang, C. J. Docherty, Q. Gao, H. H. Tan, C. Jagadish, L. M. Herz, and M. B. Johnston, "Electron mobilities approaching bulk limits in "surface-free" GaAs nanowires," Nano Lett. **14**, 5989 (2014).
[172]H. Zhang, G. Jacopin, V. Neplokh, L. Largeau, F. H. Julien, O. Kryliouk, and M. Tchernycheva, "Color control of nanowire InGaN/GaN light emitting diodes by post-growth treatment," Nanotechnology **26**, 465203 (2015).
[173]V. Piazza, M. Vettori, A. A. Ahmed, P. Lavenus, F. Bayle, N. Chauvin, F. H. Julien, P. Regreny, G. Patriarche, A. Fave, M. Gendry, and M. Tchernycheva,

Published under license by AIP Publishing

"Nanoscale investigation of a radial p–n junction in self-catalyzed GaAs nanowires grown on Si(111)," Nanoscale **10**, 20207 (2018).
[174]F. Donatini and J. Pernot, "Exciton diffusion coefficient measurement in ZnO nanowires under electron beam irradiation," Nanotechnology **29**, 105703 (2018).
[175]D. E. Ioannou and C. A. Dimitriadis, "A SEM-EBIC minority-carrier diffusion-length measurement technique," IEEE Trans. Electron Devices **29**, 445 (1982).
[176]C. Donolato, "Evaluation of diffusion lengths and surface recombination velocities from electron beam induced current scans," Appl. Phys. Lett. **43**, 120 (1983).
[177]E. B. Yakimov, S. S. Borisov, and S. I. Zaitsev, "EBIC measurements of small diffusion length in semiconductor structures," Semiconductors **41**, 411–413 (2007).
[178]O. Saket, C. Himwas, V. Piazza, F. Bayle, A. Cattoni, F. Oehler, G. Patriarche, L. Travers, S. Collin, F. H. Julien, J.-C. Harmand, and M. Tchernycheva, "Nanoscale electrical analyses of axial-junction GaAsP nanowires for solar cell applications," Nanotechnology **31**, 145708 (2020).
[179]V. Piazza, S. Wirths, N. Bologna, A. A. Ahmed, F. Bayle, H. Schmid, F. Julien, and M. Tchernycheva, "Nanoscale analysis of electrical junctions in InGaP nanowires grown by template-assisted selective epitaxy," Appl. Phys. Lett. **114**, 103101 (2019).
[180]H.-L. Chen, C. Himwas, A. Scaccabarozzi, P. Rale, F. Oehler, A. Lemaître, L. Lombez, J.-F. Guillemoles, M. Tchernycheva, J.-C. Harmand, A. Cattoni, and S. Collin, "Determination of N-type doping level in single GaAs nanowires by cathodoluminescence," Nano Lett. **17**, 6667 (2017).
[181]M. Vettori, V. Piazza, A. Cattoni, A. Scaccabarozzi, G. Patriarche, P. Regreny, N. Chauvin, C. Botella, G. Grenet, J. Penuelas, A. Fave, M. Tchernycheva, and M. Gendry, "Growth optimization and characterization of regular arrays of GaAs/AlGaAs core/shell nanowires for tandem solar cells on silicon," Nanotechnology **30**, 084005 (2019).
[182]M. Tchernycheva, V. Neplokh, H. Zhang, P. Lavenus, L. Rigutti, F. Bayle, F. H. Julien, A. Babichev, G. Jacopin, L. Largeau, R. Ciechonski, G. Vescovi, and O. Kryliouk, "Core–shell InGaN/GaN nanowire light emitting diodes analyzed by electron beam induced current microscopy and cathodoluminescence mapping," Nanoscale **7**, 11692 (2015).
[183]M. T. Borgstrom, M. H. Magnusson, F. Dimroth, G. Siefer, O. Hohn, H. Riel, H. Schmid, S. Wirths, M. Bjork, I. Aberg, W. Peijnenburg, M. Vijver, M. Tchernycheva, V. Piazza, and L. Samuelson, "Towards nanowire tandem junction solar cells on silicon," IEEE Journal of Photovoltaics **8**(3), 733 (2018).
[184]J. Bolinsson, M. Ek, J. Trägårdh, K. Mergenthaler, D. Jacobsson, M.-E. Pistol, L. Samuelson, and A. Gustafsson, "GaAs/AlGaAs heterostructure nanowires studied by cathodoluminescence," Nano Res. **7**, 473 (2014).
[185]G. Nogues, T. Auzelle, M. Den Hertog, B. Gayral, and B. Daudin, "Cathodoluminescence of stacking fault bound excitons for local probing of the exciton diffusion length in single GaN nanowires," Appl. Phys. Lett. **104**, 102102 (2014).
[186]M. Kociak and L. F. Zagonel, "Cathodoluminescence in the scanning transmission electron microscope," Ultramicroscopy **176**, 112 (2017).
[187]D. Lindgren, O. Hultin, M. Heurlin, K. Storm, M. T. Borgström, L. Samuelson, and A. Gustafsson, "Study of carrier concentration in single InP nanowires by luminescence and Hall measurements," Nanotechnology **26**, 045705 (2015).
[188]D. Wolf, R. Hübner, T. Niermann, S. Sturm, P. Prete, N. Lovergine, B. Büchner, and A. Lubk, "Three-dimensional composition and electric potential mapping of III–V core–multishell nanowires by correlative STEM and holographic tomography," Nano Lett. **18**, 4777 (2018).
[189]W. Choi, E. Seabron, P. K. Mohseni, J. D. Kim, T. Gokus, A. Cernescu, P. Pochet, H. T. Johnson, W. L. Wilson, and X. Li, "Direct electrical probing of periodic modulation of zinc-dopant distributions in planar gallium arsenide nanowires," ACS Nano **11**, 1530 (2017).
[190]A. Troian, G. Otnes, X. Zeng, L. Chayanun, V. Dagytė, S. Hammarberg, D. Salomon, R. Timm, A. Mikkelsen, M. T. Borgström, and J. Wallentin, "Nanobeam x-ray fluorescence dopant mapping reveals dynamics of in situ Zn-doping in nanowires," Nano Lett. **18**, 6461 (2018).
[191]S. Hertenberger, D. Rudolph, M. Bichler, J. J. Finley, G. Abstreiter, and G. Koblmüller, "Growth kinetics in position-controlled and catalyst-free InAs nanowire arrays on Si(111) grown by selective area molecular beam epitaxy," J. Appl. Phys. **108**, 114316 (2010).
[192]V. G. Dubrovskii, T. Xu, A. D. Álvarez, S. R. Plissard, P. Caroff, F. Glas, and B. Grandidier, "Self-equilibration of the diameter of Ga-catalyzed GaAs nanowires," Nano Lett. **15**, 5580 (2015).
[193]P. Schroth, M. Al Humaidi, L. Feigl, J. Jakob, A. Al Hassan, A. Davtyan, H. Küpers, A. Tahraoui, L. Geelhaar, U. Pietsch, and T. Baumbach, "Impact of the shadowing effect on the crystal structure of patterned self-catalyzed GaAs nanowires," Nano Lett. **19**, 4263 (2019).
[194]E. K. Mårtensson, S. Lehmann, K. A. Dick, and J. Johansson, "Effect of radius on crystal structure selection in III–V nanowire growth," Cryst. Growth Des. **20**, 5373 (2020).
[195]K. A. Dick, P. Caroff, J. Bolinsson, M. E. Messing, J. Johansson, K. Deppert, L. R. Wallenberg, and L. Samuelson, "Control of III–V nanowire crystal structure by growth parameter tuning," Semicond. Sci. Technol. **25**, 024009 (2010).
[196]D. Rudolph, L. Schweickert, S. Morkötter, B. Loitsch, S. Hertenberger, J. Becker, M. Bichler, G. Abstreiter, J. J. Finley, and G. Koblmüller, "Effect of interwire separation on growth kinetics and properties of site-selective GaAs nanowires," Appl. Phys. Lett. **105**, 033111 (2014).
[197]M. T. Borgström, G. Immink, B. Ketelaars, R. Algra, and E. P. A. M. Bakkers, "Synergetic nanowire growth," Nat. Nanotechnol. **2**, 541 (2007).
[198]M. Heiss, E. Russo-Averchi, A. Dalmau-Mallorquí, G. Tütüncüoğlu, F. Matteini, D. Rüffer, S. Conesa-Boj, O. Demichel, E. Alarcon-Lladó, and A. Fontcuberta i Morral, "III–V nanowire arrays: Growth and light interaction," Nanotechnology **25**, 014015 (2014).
[199]A. Dorodnyy, E. Alarcon-Lladó, V. Shklover, C. Hafner, A. Fontcuberta i Morral, and J. Leuthold, "Efficient multiterminal spectrum splitting via a nanowire array solar cell," ACS Photonics **2**, 1284 (2015).
[200]W.-B. Jung, S. Jang, S.-Y. Cho, H.-J. Jeon, and H.-T. Jung, "Recent progress in simple and cost-effective top-down lithography for ≈10 Nm scale nanopatterns: From edge lithography to secondary sputtering lithography," Adv. Mater. **32**, 1907101 (2020).
[201]T. Karzig, C. Knapp, R. M. Lutchyn, P. Bonderson, M. B. Hastings, C. Nayak, J. Alicea, K. Flensberg, S. Plugge, Y. Oreg, C. M. Marcus, and M. H. Freedman, "Scalable designs for quasiparticle-poisoning-protected topological quantum computation with Majorana zero modes," Phys. Rev. B **95**, 235305 (2017).
[202]R. M. Lutchyn, E. P. A. M. Bakkers, L. P. Kouwenhoven, P. Krogstrup, C. M. Marcus, and Y. Oreg, "Majorana zero modes in superconductor–semiconductor heterostructures," Nat. Rev. Mater. **3**, 52 (2018).
[203]L. Shen, E. Y. B. Pun, and J. C. Ho, "Recent developments in III–V semiconducting nanowires for high-performance photodetectors," Mater. Chem. Front. **1**, 630 (2017).
[204]M. Fahed, L. Desplanque, D. Troadec, G. Patriarche, and X. Wallart, "Selective area heteroepitaxy of GaSb on GaAs (001) for in-plane InAs nanowire achievement," Nanotechnology **27**, 505301 (2016).
[205]M. Friedl, K. Cerveny, P. Weigele, G. Tütüncüoglu, S. Martí-Sánchez, C. Huang, T. Patlatiuk, H. Potts, Z. Sun, M. O. Hill, L. Güniat, W. Kim, M. Zamani, V. G. Dubrovskii, J. Arbiol, L. J. Lauhon, D. M. Zumbühl, and A. Fontcuberta i Morral, "Template-assisted scalable nanowire networks," Nano Lett. **18**, 2666 (2018).
[206]F. Krizek, J. E. Sestoft, P. Aseev, S. Marti-Sanchez, S. Vaitiekėnas, L. Casparis, S. A. Khan, Y. Liu, T. Stankevič, A. M. Whiticar, A. Fursina, F. Boekhout, R. Koops, E. Uccelli, L. P. Kouwenhoven, C. M. Marcus, J. Arbiol, and P. Krogstrup, "Field effect enhancement in buffered quantum nanowire networks," Phys. Rev. Mater. **2**, 093401 (2018).
[207]L. Desplanque, A. Bucamp, D. Troadec, G. Patriarche, and X. Wallart, "Selective area molecular beam epitaxy of InSb nanostructures on mismatched substrates," J. Cryst. Growth **512**, 6 (2019).
[208]P. Aseev, A. Fursina, F. Boekhout, F. Krizek, J. E. Sestoft, F. Borsoi, S. Heedt, G. Wang, L. Binci, S. Martí-Sánchez, T. Swoboda, R. Koops, E. Uccelli, J. Arbiol, P. Krogstrup, L. P. Kouwenhoven, and P. Caroff, "Selectivity map for molecular beam epitaxy of advanced III–V quantum nanowire networks," Nano Lett. **19**, 218 (2019).
[209]J. S. Lee, S. Choi, M. Pendharkar, D. J. Pennachio, B. Markman, M. Seas, S. Koelling, M. A. Verheijen, L. Casparis, K. D. Petersson, I. Petkovic, V. Schaller, M. J. W. Rodwell, C. M. Marcus, P. Krogstrup, L. P. Kouwenhoven,

Published under license by AIP Publishing

E. P. A. M. Bakkers, and C. J. Palmstrøm, "Selective-area chemical beam epitaxy of in-plane InAs one-dimensional channels grown on InP(001), InP(111)B, and InP(011) surfaces," Phys. Rev. Mater. **3**, 084606 (2019).
[210] R. L. M. Op het Veld, D. Xu, V. Schaller, M. A. Verheijen, S. M. E. Peters, J. Jung, C. Tong, Q. Wang, M. W. A. de Moor, B. Hesselmann, K. Vermeulen, J. D. S. Bommer, J. Sue Lee, A. Sarikov, M. Pendharkar, A. Marzegalli, S. Koelling, L. P. Kouwenhoven, L. Miglio, C. J. Palmstrøm, H. Zhang, and E. P. A. M. Bakkers, "In-plane selective area InSb–Al nanowire quantum networks," Commun. Phys. **3**, 59 (2020).
[211] M. Borg, H. Schmid, K. E. Moselund, G. Signorello, L. Gignac, J. Bruley, C. Breslin, P. Das Kanungo, P. Werner, and H. Riel, "Vertical III–V nanowire device integration on Si(100)," Nano Lett. **14**, 1914 (2014).
[212] H. Schmid, M. Borg, K. Moselund, L. Gignac, C. M. Breslin, J. Bruley, D. Cutaia, and H. Riel, "Template-assisted selective epitaxy of III–V nanoscale devices for co-planar heterogeneous integration with Si," Appl. Phys. Lett. **106**, 233101 (2015).
[213] M. Borg, H. Schmid, K. E. Moselund, D. Cutaia, and H. Riel, "Mechanisms of template-assisted selective epitaxy of InAs nanowires on Si," J. Appl. Phys. **117**, 144303 (2015).
[214] S. Funk, M. Royo, I. Zardo, D. Rudolph, S. Morkötter, B. Mayer, J. Becker, A. Bechtold, S. Matich, M. Döblinger, M. Bichler, G. Koblmüller, J. J. Finley, A. Bertoni, G. Goldoni, and G. Abstreiter, "High mobility one- and two-dimensional electron systems in nanowire-based quantum heterostructures," Nano Lett. **13**, 6189 (2013).
[215] J. Jadczak, P. Plochocka, A. Mitioglu, I. Breslavetz, M. Royo, A. Bertoni, G. Goldoni, T. Smolenski, P. Kossacki, A. Kretinin, H. Shtrikman, and D. K. Maude, "Unintentional high-density p-type modulation doping of a GaAs/AlAs core–multishell nanowire," Nano Lett. **14**, 2807 (2014).
[216] F. Buscemi, M. Royo, G. Goldoni, and A. Bertoni, "Tailoring the core electron density in modulation-doped core−multi-shell nanowires," Nanotechnology **27**, 195201 (2016).
[217] D. M. Irber, J. Seidl, D. J. Carrad, J. Becker, N. Jeon, B. Loitsch, J. Winnerl, S. Matich, M. Döblinger, Y. Tang, S. Morkötter, G. Abstreiter, J. J. Finley, M. Grayson, L. J. Lauhon, and G. Koblmüller, "Quantum transport and sub-band structure of modulation-doped GaAs/AlAs Core–superlattice nanowires," Nano Lett. **17**, 4886 (2017).
[218] M. Royo, M. De Luca, R. Rurali, and I. Zardo, "A review on III–V core–multi-shell nanowires: Growth, properties, and applications," J. Phys. D: Appl. Phys. **50**, 143001 (2017).
[219] S. Fust, A. Faustmann, D. J. Carrad, J. Bissinger, B. Loitsch, M. Döblinger, J. Becker, G. Abstreiter, J. J. Finley, and G. Koblmüller, "Quantum-confinement-enhanced thermoelectric properties in modulation-doped GaAs–AlGaAs core–shell nanowires," Adv. Mater. **32**, 1905458 (2020).
[220] N. Jamond, P. Chrétien, F. Houzé, L. Lu, L. Largeau, O. Maugain, L. Travers, J. C. Harmand, F. Glas, E. Lefeuvre, M. Tchernycheva, and N. Gogneau, "Piezo-generator integrating a vertical array of GaN nanowires," Nanotechnology **27**, 325403 (2016).
[221] N. Jegenyes, M. Morassi, P. Chrétien, L. Travers, L. Lu, F. Julien, M. Tchernycheva, F. Houzé, and N. Gogneau, "High piezoelectric conversion properties of axial InGaN/GaN nanowires," Nanomaterials **8**, 367 (2018).
[222] V. Piazza, A. V. Babichev, L. Mancini, M. Morassi, P. Quach, F. Bayle, L. Largeau, F. H. Julien, P. Rale, S. Collin, J.-C. Harmand, N. Gogneau, and M. Tchernycheva, "Investigation of GaN nanowires containing AlN/GaN multiple quantum discs by EBIC and CL techniques," Nanotechnology **30**, 214006 (2019).
[223] J. Lähnemann, A. Ajay, M. I. den Hertog, and E. Monroy, "Near-infrared intersubband photodetection in GaN/AlN nanowires," Nano Lett. **17**, 6954 (2017).
[224] L. Rigutti, G. Jacopin, L. Largeau, E. Galopin, A. De Luna Bugallo, F. H. Julien, J.-C. Harmand, F. Glas, and M. Tchernycheva, "Correlation of optical and structural properties of GaN/AlN core-shell nanowires," Phys. Rev. B **83**, 155320 (2011).
[225] X. Zeng, G. Otnes, M. Heurlin, R. T. Mourão, and M. T. Borgström, "InP/GaInP nanowire tunnel diodes," Nano Res. **11**, 2523 (2018).
[226] N. Bologna, S. Wirths, L. Francaviglia, M. Campanini, H. Schmid, V. Theofylaktopoulos, K. E. Moselund, A. Fontcuberta i Morral, R. Erni, H. Riel, and M. D. Rossell, "Dopant-induced Modifications of $Ga_xIn_{(1-x)}$ P nanowire-based p-n junctions monolithically integrated on Si (111)," ACS Appl. Mater. Interfaces **10**, 32588 (2018).
[227] H. Zhang, X. Dai, N. Guan, A. Messanvi, V. Neplokh, V. Piazza, M. Vallo, C. Bougerol, F. H. Julien, and A. Babichev, "Flexible photodiodes based on nitride core/shell p–n junction nanowires," ACS Appl. Mater. Interfaces **8**, 26198 (2016).
[228] L. Francaviglia, Y. Fontana, S. Conesa-Boj, G. Tütüncüoglu, L. Duchêne, M. B. Tanasescu, F. Matteini, and A. Fontcuberta i Morral, "Quantum dots in the GaAs/Al_xGa_{1-x}As core-shell nanowires: Statistical occurrence as a function of the shell thickness," Appl. Phys. Lett. **107**, 033106 (2015).
[229] J. Johansson and K. A. Dick, "Recent advances in semiconductor nanowire heterostructures," CrystEngComm **13**, 7175 (2011).
[230] S. Petrosyan, A. Yesayan, and S. Nersesyan, "Theory of nanowire radial p-n-junction," Int. J. Math. Phys. Sci. **71**, 1065 (2012).
[231] H. Zhang, N. Guan, V. Piazza, A. Kapoor, C. Bougerol, F. H. Julien, A. V. Babichev, N. Cavassilas, M. Bescond, F. Michelini, M. Foldyna, E. Gautier, C. Durand, J. Eymery, and M. Tchernycheva, "Comprehensive analyses of core–-shell InGaN/GaN single nanowire photodiodes," J. Phys. D: Appl. Phys. **50**, 484001 (2017).
[232] T. Bryllert, L. Samuelson, L. E. Jensen, and L.-E. Wernersson, "Vertical high mobility wrap-gated InAs nanowire transistor," IEEE Electron Device Lett. **27**, 323–325 (2006).
[233] T. Thingujam, D.-H. Son, J.-G. Kim, S. Cristoloveanu, and J.-H. Lee, "Effects of interface traps and self-heating on the performance of GAA GaN vertical nanowire MOSFET," IEEE Trans. Electron Devices **67**, 816 (2020).
[234] M. C. Plante and R. R. LaPierre, "Analytical description of the metal-assisted growth of III–V nanowires: Axial and radial growths," J. Appl. Phys. **105**, 114304 (2009).
[235] A. Darbandi, J. C. McNeil, A. Akhtari-Zavareh, S. P. Watkins, and K. L. Kavanagh, "Direct Measurement of the electrical abruptness of a nanowire p–n junction," Nano Lett. **16**, 3982 (2016).
[236] J. D. Christesen, C. W. Pinion, X. Zhang, J. R. McBride, and J. F. Cahoon, "Encoding abrupt and uniform dopant profiles in vapor–liquid–solid nanowires by suppressing the reservoir effect of the liquid catalyst," ACS Nano **8**, 11790 (2014).
[237] V. G. Dubrovskii, A. A. Koryakin, and N. V. Sibirev, "Understanding the composition of Ternary III-V nanowires and axial nanowire heterostructures in nucleation-limited regime," Mater. Des. **132**, 400 (2017).
[238] G. Priante, F. Glas, G. Patriarche, K. Pantzas, F. Oehler, and J.-C. Harmand, "Sharpening the interfaces of axial heterostructures in self-catalyzed AlGaAs nanowires: Experiment and theory," Nano Lett. **16**, 1917 (2016).
[239] K. A. Dick, J. Bolinsson, B. M. Borg, and J. Johansson, "Controlling the Abruptness of axial heterojunctions in III–V nanowires: Beyond the reservoir effect," Nano Lett. **12**, 3200 (2012).
[240] L. F. Zagonel, L. Rigutti, M. Tchernycheva, G. Jacopin, R. Songmuang, and M. Kociak, "Visualizing highly localized luminescence in GaN/AlN heterostructures in nanowires," Nanotechnology **23**, 455205 (2012).
[241] P. Lavenus, A. Messanvi, L. Rigutti, A. De Luna Bugallo, H. Zhang, F. Bayle, F. H. Julien, J. Eymery, C. Durand, and M. Tchernycheva, "Experimental and theoretical analysis of transport properties of core–shell wire light emitting diodes probed by electron beam induced current microscopy," Nanotechnology **25**, 255201 (2014).
[242] M. Yao, S. Cong, S. Arab, N. Huang, M. L. Povinelli, S. B. Cronin, P. D. Dapkus, and C. Zhou, "Tandem solar cells using GaAs nanowires on Si: Design, fabrication, and observation of voltage addition," Nano Lett. **15**, 7217 (2015).
[243] L. Esaki, "New phenomenon in narrow germanium p−n junctions," Phys. Rev. **109**, 603 (1958).
[244] W. Guter and A. W. Bett, "I–V characterization of tunnel diodes and multi-junction solar cells," IEEE Trans. Electron Devices **53**, 2216 (2006).
[245] A. T. M. G. Sarwar, B. J. May, J. I. Deitz, T. J. Grassman, D. W. McComb, and R. C. Myers, "Tunnel junction enhanced nanowire ultraviolet light emitting diodes," Appl. Phys. Lett. **107**, 101103 (2015).
[246] J. Bauer, F. Fleischer, O. Breitenstein, L. Schubert, P. Werner, U. Gösele, and M. Zacharias, "Electrical properties of nominally undoped silicon nanowires grown by molecular-beam epitaxy," Appl. Phys. Lett. **90**, 012105 (2007).
[247] E. P. A. M. Bakkers, J. A. van Dam, S. De Franceschi, L. P. Kouwenhoven, M. Kaiser, M. Verheijen, H. Wondergem, and P. van der Sluis, "Epitaxial growth of InP nanowires on germanium," Nat. Mater. **3**, 769 (2004).

Published under license by AIP Publishing

[248]R. Kim, U. E. Avci, and I. A. Young, "Source/drain doping effects and performance analysis of ballistic III-V n-MOSFETs," IEEE J. Electron Devices Soc. **3**, 37 (2015).
[249]A. C. Ford, S. Chuang, J. C. Ho, Y.-L. Chueh, Z. Fan, and A. Javey, "Patterned P-doping of InAs nanowires by gas-phase surface diffusion of Zn," Nano Lett. **10**, 509 (2010).
[250]H.-Y. Li, O. Wunnicke, M. T. Borgström, W. G. G. Immink, M. H. M. van Weert, M. A. Verheijen, and E. P. A. M. Bakkers, "Remote P-doping of InAs nanowires," Nano Lett. **7**, 1144 (2007).
[251]M. Friedl, K. Cerveny, C. Huang, D. Dede, M. Samani, M. O. Hill, N. Morgan, W. Kim, L. Güniat, J. Segura-Ruiz, L. J. Lauhon, D. M. Zumbühl, and A. Fontcuberta i Morral, "Remote doping of scalable nanowire branches," Nano Lett. **20**, 3577 (2020).
[252]R. R. LaPierre, A. C. E. Chia, S. J. Gibson, C. M. Haapamaki, J. Boulanger, R. Yee, P. Kuyanov, J. Zhang, N. Tajik, N. Jewell, and K. M. A. Rahman, "III-V nanowire photovoltaics: Review of design for high efficiency," Phys. Status Solidi RRL **7**, 815 (2013).
[253]V. E. Degtyarev, S. V. Khazanova, and N. V. Demarina, "Features of electron gas in InAs nanowires imposed by interplay between nanowire geometry, doping and surface states," Sci. Rep. **7**, 3411 (2017).
[254]M. Speckbacher, J. Treu, T. J. Whittles, W. M. Linhart, X. Xu, K. Saller, V. R. Dhanak, G. Abstreiter, J. J. Finley, T. D. Veal, and G. Koblmüller, "Direct Measurements of fermi level pinning at the surface of intrinsically N-type InGaAs nanowires," Nano Lett. **16**, 5135 (2016).
[255]N. Han, F. Wang, J. J. Hou, F. Xiu, S. Yip, A. T. Hui, T. Hung, and J. C. Ho, "Controllable p–n switching behaviors of GaAs nanowires via an interface effect," ACS Nano **6**, 4428 (2012).
[256]V. L. Berkovits, V. P. Ulin, M. Losurdo, P. Capezzuto, G. Bruno, G. Perna, and V. Capozzi, "Wet chemical nitridation of GaAs (100) by hydrazine solution for surface passivation," Appl. Phys. Lett. **80**, 3739 (2002).
[257]P. A. Alekseev, M. S. Dunaevskiy, V. P. Ulin, T. V. Lvova, D. O. Filatov, A. V. Nezhdanov, A. I. Mashin, and V. L. Berkovits, "Nitride surface passivation of GaAs nanowires: Impact on surface state density," Nano Lett. **15**, 63 (2015).
[258]C. Himwas, S. Collin, P. Rale, N. Chauvin, G. Patriarche, F. Oehler, F. H. Julien, L. Travers, J.-C. Harmand, and M. Tchernycheva, "*In situ* passivation of GaAsP nanowires," Nanotechnology **28**, 495707 (2017).
[259]V. Dhaka, A. Perros, S. Naureen, N. Shahid, H. Jiang, J.-P. Kakko, T. Haggren, E. Kauppinen, A. Srinivasan, and H. Lipsanen, "Protective capping and surface passivation of III-V nanowires by atomic layer deposition," AIP Adv. **6**, 015016 (2016).
[260]F. Gonzàlez-Posada, R. Songmuang, M. D. Hertog, and E. Monroy, "Room-temperature photodetection dynamics of single GaN nanowires," Nano Lett. **12**, 172 (2012).
[261]M. Spies, M. I. den Hertog, P. Hille, J. Schörmann, J. Polaczyński, B. Gayral, M. Eickhoff, E. Monroy, and J. Lähnemann, "Bias-controlled spectral response in GaN/AlN single-nanowire ultraviolet photodetectors," Nano Lett. **17**, 4231 (2017).
[262]F. González-Posada, R. Songmuang, M. D. Hertog, and E. Monroy, "Environmental sensitivity of n-i-n and undoped single GaN nanowire photodetectors," Appl. Phys. Lett. **102**, 213113 (2013).
[263]B. Connors, M. Povolotskyi, R. Hicks, and B. Klein, "Simulation and design of core-shell GaN nanowire LEDs," Proc. SPIE **7597**, 75970B (2010).
[264]X. Guo and E. F. Schubert, "Current crowding in GaN/InGaN light emitting diodes on insulating substrates," J. Appl. Phys. **90**, 4191 (2001).

Published under license by AIP Publishing